KINETICS OF ULTRAVIOLET B IRRADIATION-MEDIATED REACTIVE OXYGEN SPECIES GENERATION IN HUMAN KERATINOCYTES

Miss Apiriya Dhumrongvaraporn

A Thesis Submitted in Partial Fulfillment of the Requirements
for the Degree of Master of Science Program in Pharmaceutical Technology
Department of Pharmaceutics and Industrial Pharmacy
Faculty of Pharmaceutical Sciences
Chulalongkorn University
Academic Year 2011

จลนศาสตร์ของการเกิดอนุพันธ์ออกซิเจนที่ว่องไว

ในเซลล์เคราติโนไซต์ของมนุษย์ที่ถูกกระตุ้นด้วยรังสีอัลตราไวโอเลตบี

นางสาวอภิริญา ธำรงวราภรณ์

วิทยานิพนธ์นี้เป็นส่วนหนึ่งของการศึกษาตามหลักสูตรปริญญาวิทยาศาสตรมหาบัณฑิต
สาขาวิชาเทคโนโลยีเภสัชกรรม ภาควิชาวิทยาการเภสัชกรรมและเภสัชอุตสาหกรรม
คณะเภสัชศาสตร์ จุฬาลงกรณ์มหาวิทยาลัย
ปีการศึกษา 2554

Thesis Title	KINETICS OF ULTRAVIOLET B IRRADIATION-MEDIATED REACTIVE OXYGEN SPECIES GENERATION IN HUMAN KERATINOCYTES
By	Miss Apiriya Dhumrongvaraporn
Field of Study	Pharmaceutical Technology
Thesis Advisor	Assistant Professor Pithi Chanvorachote, Ph.D.

Accepted by the Faculty of Pharmaceutical Sciences, Chulalongkorn University in Partial Fulfillment of the Requirements for the Master's Degree

Pintip Pongpech ..... Dean of the Faculty of Pharmaceutical Sciences
(Associate Professor Pintip Pongpetch, Ph.D.)

THESIS COMMITTEE

Parkpoom Tengamnuay .....Chairman
(Associate Professor Parkpoom Tengamnuay, Ph.D.)

Pithi Chanvorachote .....Thesis Advisor
(Assistant Professor Pithi Chanvorachote, Ph.D.)

Angkana Tantituvanont .....Examiner
(Assistant Professor Angkana Tantituvanont, Ph.D.)

C. Chinpaisal .....External Examiner
(Associate Professor Chatchai Chinpaisal, Ph.D.)

อภิริญา ธำรงวราภรณ์: จลนศาสตร์ของการเกิดอนุพันธ์ออกซิเจนที่ว่องไวในเซลล์เคราติโนไซต์ของมนุษย์ที่ถูกกระตุ้นด้วยรังสีอัลตราไวโอเลตบี. (KINETICS OF ULTRAVIOLET B IRRADIATION-MEDIATED REACTIVE OXYGEN SPECIES GENERATION IN HUMAN KERATINOCYTES) อ. ที่ปรึกษาวิทยานิพนธ์หลัก: ผศ. ภก. ดร.ปิติ จันทร์วรโชติ, 110 หน้า.

ผลของรังสีอัลตราไวโอเลตบี หรือ ยูวีบี ในการกระตุ้นสภาวะเครียดออกซิเดชันในเซลล์เคราติโนไซต์เป็นปัจจัยที่สำคัญที่ทำให้ผิวหนังถูกทำลาย การศึกษานี้แสดงจลนศาสตร์ของการเกิดอนุพันธ์ออกซิเจนที่ว่องไว และ ระบุอนุพันธ์ออกซิเจนที่จำเพาะเจาะจงที่ถูกสร้างในเซลล์เคราติโนไซต์เมื่อถูกฉายด้วยรังสียูวีบี เซลล์เคราติโนไซต์ถูกฉายด้วยรังสียูวีบีที่ขนาดคลื่นต่างๆ และจลนศาสตร์ของอนุพันธ์ออกซิเจนภายในเซลล์ถูกวัดค่าโดยใช้การทดสอบอนุพันธ์ออกซิเจนที่จำเพาะเจาะจง ได้แก่ ดีซีเอฟ ดีเอชอี เอ็มเปกเร้ด และเอชพีเอฟ ผลการทดลองพบว่า เซลล์ที่ถูกฉายด้วยรังสียูวีบีแสดงการเพิ่มขึ้นของปริมาณอนุพันธ์ออกซิเจนอย่างมีนัยสำคัญที่ช่วงเวลาเริ่มต้น (0-2 ชม.) เมื่อเปรียบเทียบกับเซลล์ที่ไม่ได้ถูกฉายรังสี นอกจากนี้อนุพันธ์ออกซิเจนในเวลาถัดมา (2-6 ชม.) แสดงว่าไม่มีความแตกต่างของอนุพันธ์ออกซิเจนเมื่อเปรียบเทียบกับเซลล์ควบคุม อย่างไรก็ตามระดับอนุพันธ์ออกซิเจนที่จำเพาะเจาะจง ได้แก่ ซุปเปอร์ออกไซด์แอนไอออน ไฮโดรเจนเปอร์ออกไซด์ และ ไฮดรอกซิลเรดิเคิล ถูกกระตุ้นให้เพิ่มขึ้นในเซลล์เคราติโนไซต์ที่ถูกฉายด้วยรังสียูวีบี โดยผลการทดลองทางจลนศาสตร์ระบุว่าซุปเปอร์ออกไซด์แอนไอออน และ ไฮดรอกซิลเรดิเคิล คืออนุพันธ์ออกซิเจนที่จำเพาะเจาะจงหลักที่ทำให้เกิดสภาวะเครียดออกซิเดชัน ในช่วงเวลาเริ่มต้น (0-2 ชม.) หลังจากเซลล์ถูกกระตุ้นด้วยรังสียูวีบี นอกจากนี้ วิตามินซี วิตามินอี และ ซิริมาริน ถูกใช้เป็นสารต้านอนุมูลอิสระในการทดลองนี้ เพื่อดูผลของจลนศาสตร์อนุพันธ์ออกซิเจนในเซลล์เคราติโนไซต์ที่ถูกฉายด้วยรังสียูวีบี ผลการทดลองพบว่า สารต้านอนุมูลอิสระทั้ง 3 ชนิดสามารถลดการสร้างอนุพันธ์ออกซิเจนที่ถูกกระตุ้นโดยรังสียูวีบีในทุกช่วงเวลาการทดลอง เมื่อเปรียบเทียบกับเซลล์ที่ไม่ได้ให้สารต้านอนุมูลอิสระ ยิ่งไปกว่านั้น การวิเคราะห์ค่าความสัมพันธ์ยังพบว่า การเพิ่มขึ้นของอนุพันธ์ออกซิเจนในช่วงเวลาเริ่มต้น (0-2 ชม.) มีความสัมพันธ์กับการตายของเซลล์แบบอะพอพโตติกในเซลล์เคราติโนไซต์ งานวิจัยดังกล่าวจะเป็นข้อมูลเบื้องต้นเกี่ยวกับจลนศาสตร์อนุพันธ์ออกซิเจนที่ถูกสร้างในเซลล์เคราติโนไซต์เมื่อถูกฉายด้วยรังสียูวีบี ซึ่งจะเป็นประโยชน์ในการพัฒนากลยุทธ์แบบใหม่ๆ เพื่อป้องกันการทำลายของผิวหนัง

ภาควิชา วิทยาการเภสัชกรรมและเภสัชอุตสาหกรรม ลายมือชื่อนิสิต อภิริญา ธำรงวราภรณ์

สาขาวิชา เทคโนโลยีเภสัชกรรม ลายมือชื่อ อ.ที่ปรึกษาวิทยานิพนธ์หลัก

ปีการศึกษา 2554

5376857833 : MAJOR PHARMACEUTICAL TECHNOLOGY
KEYWORDS : ULTRAVIOLET B / HUMAN KERATINOCYTES / REACTIVE OXYGEN SPECIES

APIRIYA DHUMRONGVARAPORN : KINETICS OF ULTRAVIOLET B IRRADIATION-MEDIATED REACTIVE OXYGEN SPECIES GENERATION IN HUMAN KERATINO CYTES. ADVISOR: ASST. PROF. PITHI CHANVORACHOTE, Ph.D., 110 pp.

UVB-mediated oxidative stress in keratinocytes has been accepted as an important factor contributing to skin damages. The present study revealed the kinetics of ROS production and identified main specific ROS generated in human keratinocytes exposed to UVB. Keratinocytes were exposed to various doses of UVB and intracellular ROS kinetics were evaluated by specific oxidant probes, namely, $DCFH_2$-DA, DHE, Amplex Red, and HPF. Results revealed that UVB-irradiated cells exhibited significantly higher rate of ROS production in the early time period (0-2 h) compared to the non-treated control cells; however, the rate of ROS generation afterward (2-6 h) was similar to that of control cells. Specific ROS including superoxide anion, hydrogen peroxide, and hydroxyl radical were enhanced in keratinocytes treated with UVB. Results regarding kinetics of specific ROS production revealed that superoxide anion and hydroxyl radical were main ROS contributing to oxidative stress in the early phase (0-2 h) after UVB treatment in these cells. Furthermore, this study demonstrated the effect of known antioxidants vitamin C, vitamin E, and silymarin on ROS generating kinetics in UVB-exposed keratinocytes. The results indicated that all antioxidants could suppress ROS generation in response to UVB irradiation in a time-dependent manner as compared to non-antioxidant treated cells. In addition, the linear regression analysis revealed that the rate of ROS generation in early period (0-2 h) correlated with apoptotic cell death of keratinocytes. These findings revealed the novel information regarding ROS generating kinetic in UVB-exposed keratinocytes, which may benefit the development of new strategies in protecting of skin damage.

Department: Pharmaceutics and Industrial Pharmacy... Student's Signature Apiriya D.
Field of Study: ....Pharmaceutical Technology..... Advisor's Signature .....
Academic Year: .....2011.....

ACKNOWLEDGEMENTS

Firstly, I would like to express my deep appreciation to my advisor, Assistant Professor Pithi Chanvorachote for his support, guidance, and the opportunity he has given me. This thesis could not be completed and successful if without his assistance.

I would like to express my gratitude to Dr. Varisa Pongrakhananon, Mr. Preedakorn Chunhacha, Mr. Chatchai Choatham, Mr. Hasseri Halim, Mr. Wongsakorn Suchaoin, Miss Thitiporn Songserm, and my other laboratory members for their technical teaching, supporting, sharing, encouraging me in every good or bad situation, and give a very good experience and memory that help me solve and pass through any problem while I was doing this research. In particular, I would like to express my special thanks Miss Nuttida Yongsanguanchai for her help and very good friendship for the past six years in both my bachelor and master degree.

Besides, I would like to thank my beloved close friend; Miss Nuttha Assavalertson, Miss Wipada Sompong, and Miss Nuntika Luansutam for their suggestions, helpfulness, encouragement, and understanding me when I face some problem and work to my success.

Lastly, I would like to express my deepest gratitude to my family for their love, support, encouragement, understanding, and also believing in me. For my parents, without their love and understanding in every problem, I could not pass through and would not have enough strength to carry this hard work until complete and successful. For my brother and sister, I would like to thank for their encouragement and supporting.

CONTENTS

LIST OF TABLES

Page

Page

Page

LIST OF FIGURES

Page

Page

LIST OF ABBREVIATIONS

%	= percentage
°C	= degree Celsius
Amplex Red	= 10-acetyl-3, 7-dihydroxyphenoxazine
ANOVA	= analysis of variance
CO_2	= carbon dioxide
$DCFH_2$-DA	= 2,7-dichlorofluorescein diacetate
DHE	= dihydroethidium
DMEM	= dulbecco's modified Eagle's medium
DMSO	= dimethyl sulfoxide
EDTA	= ethylenediaminetetraacetic acid
et al.	= et alibi, and others
g	= gram
h	= hour, hours
H_2O_2	= hydrogen peroxide
HPF	= 3'-(p-hydroxyphenyl) fluorescein
J/m^2	= Joule per square meter
min	= minute (s)
ml	= milliliter
mM	= millimolar
MTT	= 3-(4,5-Dimethylthiazol-2-yl)-2,5-diphenyltetrazolium bromide
$O_2^{\cdot -}$	= superoxide anion radical
$^{\cdot}OH$	= hydroxyl radical
PBS	= phosphate buffer saline
PI	= propidium iodide
ROS	= reactive oxygen species
S.D.	= standard deviation
U	= unit
W/cm^2	= watt per square centimeter

CHAPTER I

INTRODUCTION

Damaging cellular components including keratinocytes and fibroblasts results in skin complications such as aging and cancer (Guo *et al*., 2010; Matito *et al*., 2011). Keratinocyte, a principle cellular component of outmost layer of skin, has been shown to be the most affected by the ultraviolet (UV) radiation (Fisher *et al*., 1996; Kraemer *et al*., 1997). Indeed, ROS like superoxide anion ($^{\bullet}O_2^-$), hydrogen peroxide (H_2O_2), and hydroxyl radical ($^{\bullet}OH$) are continuously generated in human cells along with cellular energy production via mitochondrial electron transport reaction (Kirkinezos and Moraes, 2001; Liu *et al*., 2002; Chen *et al*., 2007). Firstly, electrons leaking out of transport chain react with oxygen to form superoxide anion (Halliwell and Gutteridge, 1984; Devasagayam *et al*., 2004). Then superoxide anion is transformed by a catalytic activity of superoxide dismutase enzyme to hydrogen peroxide and in the presence of metal, hydrogen peroxide is converted to hydroxyl radical via the Fenton reaction (Halliwell and Gutteridge, 1984; Salganik, 2011). Also, glutathione peroxidase and catalase are able to detoxify hydrogen peroxide to non-reactive water. Basically, approximately 1-3% of oxygen consumed by the cells will be converted to superoxide anion; however, in response to several stimuli including UV irradiation, increased cellular ROS production is frequently occurred (Bossi *et al*., 2008). Increased levels of cellular ROS overwhelm the cellular antioxidant mechanisms, excess ROS interaction with cellular DNA, proteins, and lipids can cause significant impact on cell signaling, behaviors, and survival (Thannickal and Fanburg et al., 2000; Saitoh *et al*., 2011).

There are 3 types of solar UV radiation, UVA (315-400 nm), UVB (280-315 nm), and UVC (wavelength < 280 nm). Among these, UVB has been recognized as the most severe damaging to the epidermis layer of skin (Wang and Kochevar, 2005). In particular, UVB-mediated DNA damage through oxidative stress-dependent mechanism in keratinocyte was demonstrated in many studies (Maccubin *et al*., 1995; Lisby *et al*., 2005). Although much attempt has been made for the evaluation of cytotoxic effects caused by UVB exposure, the information involving kinetics of ROS production and in particular specific oxidative species induction after UVB exposure has not been evaluated. Study of the kinetics and species of induced ROS may help to understand the mechanism of UVB-induced cell damage and related cellular responses. In addition, vitamin C, vitamin E, and silymarin are used as an antioxidant for attenuating ROS production induced by UVB in this experiment. All antioxidants are used as an active ingredient in many commercial products available in the market.

The main focuses of this study are to investigate the ROS generating kinetics and to identify the responsible specific ROS species for cellular oxidative stress and damage in UVB-exposed keratinocytes. It has been known that UVB could induced ROS generation in skin keratinocytes; however, there is no detail regarding the type of specific ROS generated. Besides, the kinetic of ROS production in such condition is still unknown. According to the basis that the information regarding ROS producing kinetic as well as the type of ROS could render the better explanation about ROS species and time that is critical to oxidative cell damage. This information may lead to the development of more precise strategies in protecting skin cells.

The data may facilitate the development of effective strategies in attenuating undesirable effects on UV-exposed skin and may help in developing methods for

evaluation of cosmeceutical products claiming for oxidative stress and UV-relief approaches.

CHAPTER II

LITERATURE REVIEWS

Ultraviolet

Skin cancer had become one of the most dreadful skin problems known worldwide. Skin is exposed to broad variety of environmental hazards everyday, such as biological, chemical, and physical insults (Saliou *et al*., 1998). The number one environmental factor that causes many skin problems including cancer, skin aging, and immunosuppression is ultraviolet (UV) radiation. UV is a part of electromagnetic spectrum in the range between the X-ray regions and visible light. From total radiant energy from the sun received at the earth's surface , UV consist of approximately 5-10%, followed by 40% of visible light and 50% of infrared radiation (Costin and Hearing, 2007).

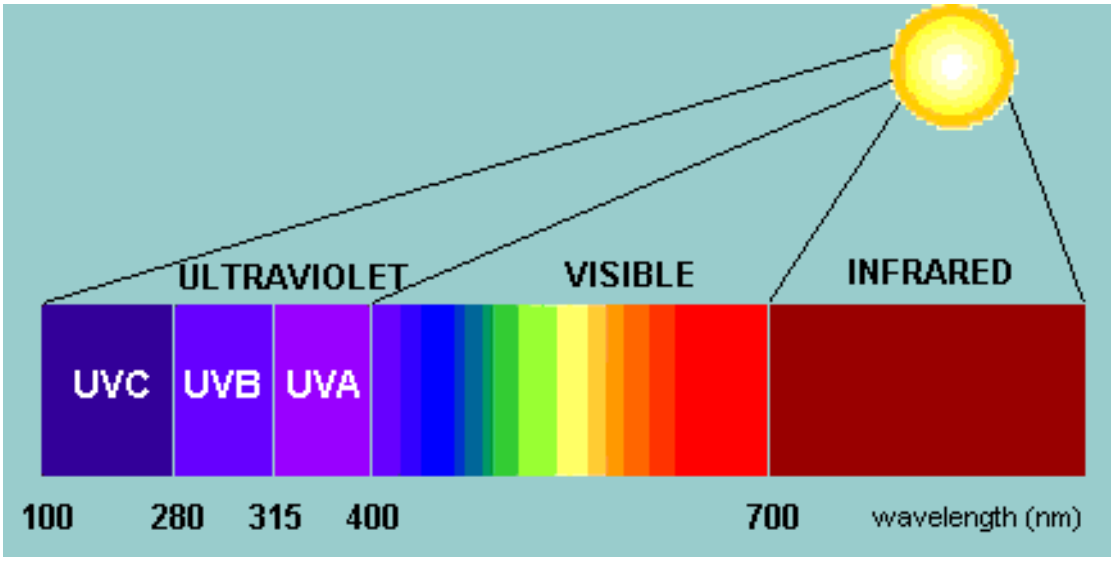

Figure 2.1 Wavelength of three ultraviolet irradiations

UVR (100-400 nm) is divided in long wavelength UVA (320-400), short wavelength UVB (290-320 nm), and UVC (100-290 nm) as show in figure 2.1. The wavelengths below 280 nm are normally screened by the ozone layer and are not allowed to reach the earth's surface (Sinha and Hader, 2002). Therefore, from these three radiations, both UVA and UVB can reach to the earth's surface, thus only UVC cannot pass through the atmospheric ozone layer.

UVA causes oxidation of cellular components such as lipids, DNA, and proteins that induced the frequent lesions. The oxygen intermediates will cause the formation of strand break and oxidized bases in DNA. Most of UVA can pass through automobiles, office, glass windows, and can also penetrate deeply into the dermis of skin approximately 19-50% (Garland C, Garland F, and Gorham, 1993). In contrast, UVB is blocked by glass window and only 9-14% of solar UVB can reach the depth of melanocytes (Costin and Hearing, 2007). UVB absorbed to the epidermis and upper dermis of the skin is responsible for causing sunburn reaction, induction of cyclobutane pyramidine dimer (CPD) (Lehmann *et al*., 1998), lipid peroxidation, and an accurate inflammatory response. Moreover, the production of melanin is stimulated by UVB. This may be associated with increase risk of skin cancer if the UV exposure has been prolonged and repeated (Costin and Hearing, 2007).

UVB radiation damages keratinocyte DNA by suppressing the immune system, cutaneous malignancy, non-melanoma skin cancer, and induction chronic skin damage. UVB exposure can induce DNA damage both directly and indirectly (Cunningham *et al*., 1985; Hattori *et al*., 1996). Direct damage to DNA occurs from the formation of cyclobutane-pyrimidine dimers and 6-4 pyrimidine-pyrimidone

photoproducts, while indirect DNA damage leads to up-regulation in the level of reactive oxygen species that simplify DNA oxidation.

Interestingly, it has been vastly reported that UVB radiation mediates the production of ROS and induces stimulation of some specific signal transduction pathways leading to cell death, cell cycle progression arrest, as well as altered gene expression (Tyrrell, 1995; Bender *et al*., 1997; Scharffetter-Kochanek *et al*., 1997).

Reactive Oxygen Species

Reactive oxygen species (ROS) are constantly produced within cell or mammalian tissues by mitochondria via the release of electron from mitochondria electron transport chain and the redox reactions implicating electron transfer group such as their phenolic precursors, quinolones, some metal complexes, conjugated imines, and aromatic nitro compounds (Heck *et al*., 2003). Normally, the formation of ROS occurs in the cells by two ways, which are enzymatic and non-enzymatic reaction. Most cells generated three main types of ROS, namely superoxide anion ($O_2^{\bullet}$), hydrogen peroxide (H_2O_2), and hydroxyl radical ($OH^{\bullet}$). Among them, superoxide and hydrogen peroxide is the cellular ROS that are the most aggressive entity.

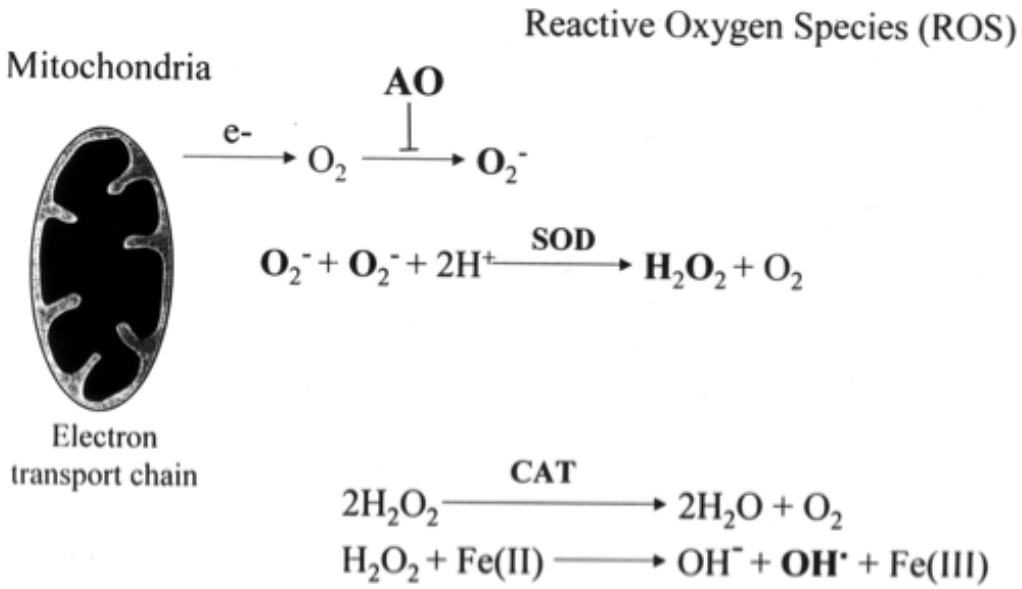

Figure 2.2 Reactive Oxygen Species (ROS)

Superoxide is the first and main cellular ROS that produced from non-enzymatic process, generated in mitochondria via electron released from electron transport chain and reduction of oxygen molecules to superoxide to form superoxide anion radical. Even though, superoxide anion radical is unable to penetrate in lipid membranes, the two molecules of superoxide anion radical rapidly form hydrogen peroxide (H_2O_2) via superoxide dismutase (SOD), which is able to penetrate easily to the cell membranes. Hydrogen peroxide acts as inter or intracellular signaling molecule and is able to cross in the cell membrane, so hydrogen peroxide can react with some antioxidant enzyme such as catalase and glutathione peroxidase to form water. While, some of hydrogen peroxide atom would react with metal ions, namely (Fe^{2+} or Cu^{+}) to generate the hydroxyl radical ($^{\cdot}OH$) in the cell via Fenton reaction, very toxicity and reactive than other ROS as shown in figure 2.2. However, superoxide anion radical and hydrogen peroxide occurred intermediate reaction with

some metal ions (Fe^{2+} or Cu^{+}) via reduction of metal ions (Thannickal and Fanburg, 2000; Devasagayam *et al.*, 2004). These two reactions are called Haber-Weiss reaction as demonstrated below.

Fenton reaction: $H_2O_2 + Fe^{2+}/Cu^{+} \longrightarrow {}^{\cdot}OH + OH^{-} + Fe^{3+} / Cu^{2+}$

Reduction of metal ions: $O_2^{\cdot -} + Fe^{3+} / Cu^{2+} \longrightarrow O_2 + Fe^{2+}/Cu^{+}$

Haber-Weiss reaction: $H_2O_2 + O_2^{\cdot -} \longrightarrow {}^{\cdot}OH + OH^{-} + O_2$

The concentration of ROS is very important to the function of the cell. The low or moderate ROS level can be useful for biological molecular functions, whereas the high concentration of ROS will be harmful and cause danger to cells. The overproduction of ROS production may lead to oxidative stress, which the formation of ROS and antioxidant defenses are imbalance. The excess of ROS in the cells react with biological molecules, namely protein, lipid, lipid peroxidation, DNA and protein (Nordberg and Arner, 2001; Young and Woodside, 2001; Valko *et al.*, 2007; Pham-Huy He, and Pham-Huy C, 2008) and cause the cell death such as apoptosis and necrosis or loss of cell function.

- Lipids and lipid peroxidation

Membrane lipid exists in every subcellular organelles are highly sensitive to the free radical damage. Many previous studies has been provided that lipid interact with free radical can undergo the highly damaging chain reaction of lipid peroxidation (LP) in both direct and indirect effects, especially produced hydroxyl radical. According to the plasma membrane it damage and cause further oxidation of membrane resulting in cell injury (Gutteridge, 1982; Teiero *et al.*, 2007).

- DNA

The excess ROS will react with DNA and resulting in the oxidative damage in our body. It not only causes DNA damage, but also inhibit DNA-repairing process in the cells, which implicated in carcinogenesis and mutagenesis (Marnett, 2000; Nordberg and Arner, 2001; Devasagayam *et al*., 2004).

- Protein

The structural change and enzyme inactivation in the cells such as DNA repairing enzyme, membrane transporter proteins, and DNA polymerase occurred from the excess of ROS production reacted with the several amino acids like amino acids, proteins, and peptides, which develops pathophysiology of various diseases and cellular damage to the cells (Butterfield *et al*., 1998; Nordberg and Arner, 2001).

In addition, the excess ROS production effect that was induced by UVB has been reported as destroying cells function in our body including cell death, which are apoptosis and necrosis.

UVB irradiation-induced apoptosis and necrosis

UVB is the most important environmental effect that can go deep through the skin. From that effect, it may cause cell death that may represent as physical effect on skin such as sunburn. Cell death may occur by one of three paths, termed which are apoptosis, necrosis, and differentiation (Beaulaton and Lockshin, 1982; Mammone, 2000).

Apoptosis is morphologically difference form of cell death that controlled by mechanism. It can be induced by pharmacological or physiological stimuli especially by UVB (Kerr *et al*., 1972). The characteristic of apoptosis cell death is represented

by the chromatin condensation and cytoplasm, cell shrinkage, nucleus fragmentation, membrane blebbing and fragmentation of cell into apoptotic body that is phagocytized via neighboring cell (Kerr, 1971). When the normal human skin is exposed to UVB, some of keratinocytes in epidermis change into apoptotic cells that are expressed as sunburn cells. The observation of sunburn cells or apoptotic cells in human keratinocytes has been understood to mean that the apoptotic cell death is active in progressing process in the formation of the skin (Young *et al.*, 1987, Haake and Polakowska, 1993).

Figure 2.3 demonstrated the pathways involved apoptosis program induced by UV. DNA damage in nucleus is induced via activation of p53 that cause apoptosis in cells. In addition, UV stimulates death receptors via induction of increase or release of death ligands revealed on the cell surface. However, UV also directly stimulates death receptors in the ligands-independent way via induce receptor clustering. Motivated the death receptors and transduce the signal of apoptotic via their intra-cytoplasmic death domain (DD). Lastly, UV also induced the release of cytochrome C in mitochondria (Kulms and Schwarz, 2000).

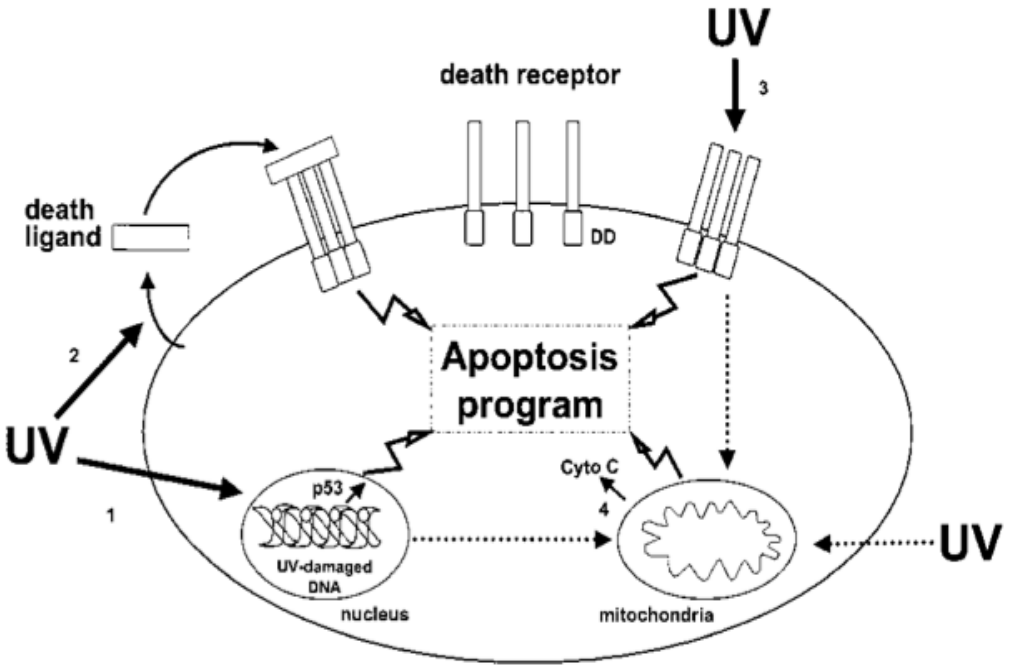

Figure 2.3 UV-induced apoptosis program

In contrast, necrosis cell death is induced by extreme damage (Caricchio, McPhie, and Cohen, 2003). It is caused by the physical pain to the cells that result in the disturbance of cell organelles and ultimately cell death that can be readily observed in the skin after exposed to the high doses of UVB (Mammone *et al*., 2000). The necrosis cell tolerates the different biochemical and morphological changes recently known to be well controlled under certain conditions (Martelli *et al*., 2001). Necrosis cells have been shown to induce an inflammatory response by the phagocytic cell, to initiate the immune response, and stimulate the expert APCs (Gallucci, Lolkema, and Matzinger, 1999; Caricchio, McPhie, and Cohen, 2003).

The normal differentiation of human skin can be supposed to a form of cell death program that result in the formation of non-metabolic, corneocyte or the differentiated of cells, and enucleated. It is lose of nucleus, mitochondria and

ribosomes in the basal cell that completely formed corneocyte in the keratinocyte progresses (Lavker and Matoltsy, 1970; Mammone *et al*., 2000).

Vitamin C

Vitamin C or ascorbic acid consists of six-carbon lactone as demonstrated in figure 2.4. It is synthesized from glucose in most mammalian liver, but not from guinea pig human, and non-human primate because these species do no have the gulonolactone oxidase enzyme which is the essential for synthesis the ascorbic acid. Vitamin C is known as a good electron donor and also a reducing agent in biochemical and physiological actions. It donates two of its electron from the double bond between the second and third carbons from the six-carbon molecule. It is remarkable that when vitamin C donates electrons to others, it is lost sequentially. The species formed of vitamin C that loss one electron is called free radical, ascorbyl radical or semidehydroascorbic acid. While vitamin C that loss two of its electron is called dehydroascorbic acid, in which its stability depends on many factors such as pH, and temperature (Washko, Wang, and Levine, 1993). Dehydroascorbic acid form may exist in several different structures, but the vitamin C dominant form *in vivo* still has not been clarified.

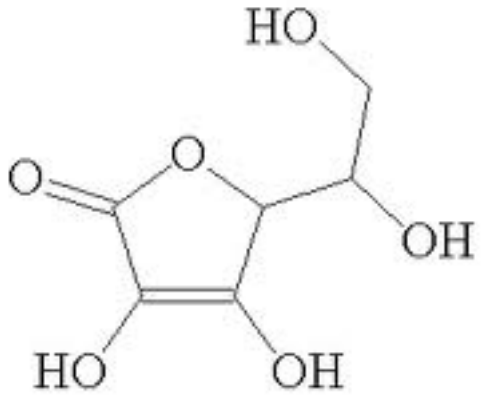

Figure 2.4 the structure of Vitamin C (ascorbic acid)

Vitamin C is a powerful water-soluble antioxidant found in intracellular and extracellular compartments due to donation of its electrons. Vitamin C can prevent others compound from being oxidized, but by the nature of reaction, vitamin C is oxidized in the process by itself. Ascorbyl radical is quite stable with half-life around 10^{-5} seconds and is fairly unreactive compared to other free radicals (the unpaired electron species). The formation of ascorbyle radical and dehydraascorbic acid are mediated by broad variety of oxidants in a biological systems, including superoxide, molecular oxygen, hypochlorous acid, hydroxyl radical, iron, copper, and reactive nitrogen specie. In a simple terms, a possibly and reactive harmful free radicals can interact with an ascorbate. Then the reactive free radicals are reduced and form the ascorbyl radical that is a less reactive compound. The formation of the less reactive compound is called quenching or free radical scavenging. However, the adcorbate is a very good free radical scavenger because of its chemical property (Bielski, Richter, and Chan, 1975; Buettner and Moseley, 1993; Sebastian *et al*., 2003).

Because of its properties, vitamin C is one important antioxidant that is used for destructing ROS that may be induced by UVB, especially hydrogen peroxide (Liebler, Kling, and Reed, 1986; Padh, 1990; Foyer, Descourvieres, and Kunert, 1994). Furthermore, vitamin C can protect two effects of UVB exposure, which are induction of cell death and up-regulation of peroxide level. However, there are many researches reported about vitamin C activity that it able to stimulate the proliferation of dermal fibroblasts in human skin and also collagen synthesis in both of collagen and monolayer lattice cultures. In addition, ascorbic acid shows very good properties that it can prevent UVB irradiation injury in human keratinocytes. As free radical generated by UVB, vitamin C scavenges peroxides and reduces the level of steady state in endogenous peroxides (Savini *et al*., 1999).

Vitamin E

Vitamin E has been discovered by Bishop and Evans as a factor of necessary dietary for rat reproduction since 1922 (Evans and Bishop, 1922; Traber and Atkinson, 2007). Vitamin E is a fat-soluble antioxidant that is a family of β-, α-, γ-, and δ-tocopherols and tocotrienols demonstrated in figure 2.6. All of them are found in various food types, but only α -tocopherol is the most active type of vitamin E that is required for human. It can protect cell membranes from oxidation via react with lipid radicals that are produced in lipid peroxidation chain reaction and ROS.

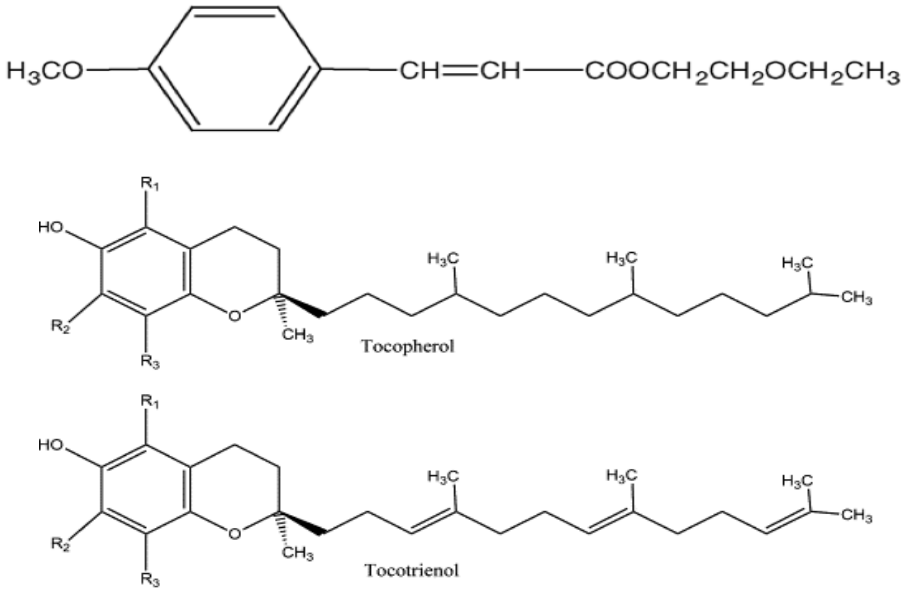

Figure 2.5 the structure of vitamin E, tocopherol and tocotrienol

Due to the facts that α –tocopherol have a higher ability to compete for the peroxyl radicals much faster than it can polyunsaturated with fatty acids. Therefore, α –tocopherol in a small amounts are able to shield polyunsaturated in a large amount. In biological membrane, the concentration of α –tocopherol is approximately 1 part/1000 of lipid molecules (Burton, Joyce, and Ingold, 1983). However, vitamin E is eventually consumed while protecting against lipid peroxidation. Though, the effectiveness of vitamin E in the lipid peroxidation effect on the living cell system is difficult and rare to obtain, some report had indicated that “pentane”, the minor product released while polyunsaturated fat peroxidation is reduced in the human supplement breath with vitamin E. These findings strongly indicated that vitamin E is superior in preventing the lipid peroxidation of the polyunsaturated fat (Lemoyne *et al*., 1987, 1988).

Antioxidant function of vitamin E is well known by many researchers as a peroxyl radical scavenger that stops chain reactions. The different form of vitamin E measured *in vitro* is very important for respecting their antioxidant activities. These consequences are due to the ability of donating H-atom of different tocols that increases in the efficiency with the greater ring of methyl substitution (Traber and Atkinson, 2007). In the actual membrane, the power of antioxidant may include the ability of H-atom donating, movement within membrane, location (penetration) plus with the recycling efficiency of tocopheroxyl radicals by the cytosolic reductant. Comparing the capacity of α-tocotrienols and α-tocopherols in the system of microsomal membrane and their antioxidant activities, results had revealed that tocotrienols is a better antioxidants in bio-membrane and is able to penetrates through the skin much faster (Suzuki *et al*., 1993).

There are many reports indicating that vitamin E shows powerful antioxidant ability in decreasing ROS production induced by UVB irradiation. Vitamin E is especially plentiful in the stratum corneum of our cells, being delivered there by the sebum. Stratum corneum is the first barrier that absorbs the oxidative stress induced by pollution and sunlight. From this exposure effect, some of vitamin E is exhausted and some of them would react with ROS induced oxidative stress by donating its phenolic hydrogen to the lipid radicals (Santa-Maria *et al*., 2010). Some researches have reported that vitamin E may act as the lipid-blocking agent that will block the lipid peroxidation chain in the cells. Surprisingly, the peak of UV absorption of vitamin E is at 295 nm, which is in the range of UVB. Therefore, photons transferred by UVB could be blocked by vitamin E for decreasing the attacks in the target of biological molecules (Jin *et al*., 2007).

Silymarin

Silymarin scientifically named *Silybum marianum*, is a flavonolignan mixture compound extracted from the Milk thistle seed. There are four flavonolignan isomers ($C_{25}H_{22}O_{11}$), including silibinin (silybin), isosilibinin (isosilybin), silydianin, and silychristin generally found in *Silybum marianum* as shown in figure 1.4. The structure of four flavonolignan isomers shown in figure 1.5. Among these flavonolignan isomers, silibinin is the major constituent of silymarin which shown the greatest degree of biology that represented around 50-60%, then 20% of silychristin, 10% of silydrianin and 5% isosilibinin respectively (Ghosh A, Ghosh T, and Jain, 2010).

Figure 2.6 Silymarin or *Silybum marianum*

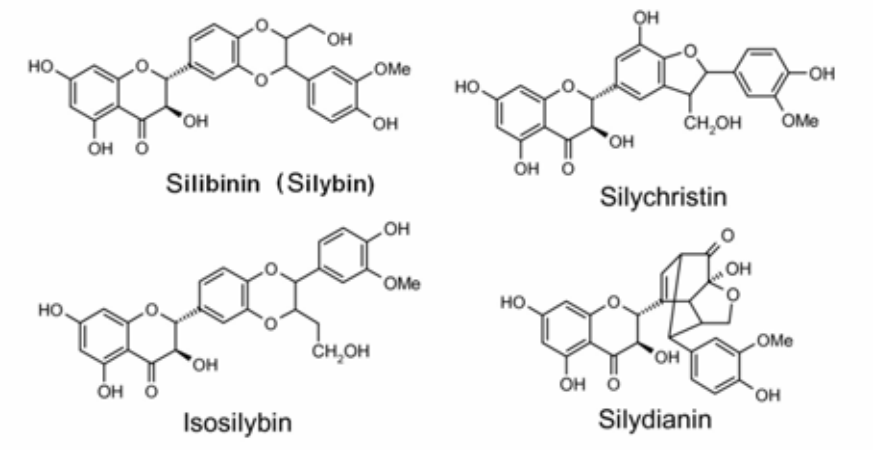

Figure 2.7 Four isomers of silymarin strutures (Sonnenbichler *et al*., 1999)

Silymarin has been known and used for more than 2000 years. It is not only used for treating many liver diseases such as hepatitis, cirrhosis, and also the disease of alcoholic liver (Flora *et al*., 1998; Saller, Meier, and Brignoli, 2001), but it also detoxify a broad range of toxic substances, for example, carbontetrachloride, halothane, galactosamine, phenylhydrazine, amanita phalloides toxin, paracetamol, erythromycin estolate and thioacetamide that are a hepatoprotective agent (Muriel *et al*., 1992; Dixit *et al*., 2007). There are many abilities of silymarin that are generally due to its pharmacological properties such as antioxidant activity, anti-inflammatory, anticancer activity and tissue regenerate stimulation.

Silymarin is not water-soluble and normally administered as an encapsulated, capsule or tablet forms that standardized extract having 70-80% of silibinin. The silibinin has an estimate half-life around 6 hours. The oral absorption approximately around 20-40% is restored from the enterohepatic circulation like sulfate conjugates and glucoronide, whereas around 3-8% is eliminated in urine (Dixit *et al*., 2007).

The antioxidant property of silymarin is ROS-scavenging and its capability to inhibit the lipid peroxidation. Many past studies suggested that silymarin is a poor scavenger in superoxide anion radicals; instead, the reaction with the hydrogen peroxide was detected. However, silymarin reacts rapidly with the hydroxyl radical and very effectively inhibits the lipid peroxidation in the system of cell-free (Velenzuela *et al*., 1985; Muriel *et al*., 1992; Asghar and Masood, 2008; Jadhav, Upasani, and Pingale, 2009). Furthermore, some toxic such as ethanol, carbontetrachloride, and paracatamol stimulate and induce lipid peroxidation in rat (Velenzuela *et al*., 1985; Muriel *et al*., 1992) as well as ultraviolet radiation, especially UVB mediated oxidative stress in human keratinocyte is prevented by silymarin. In addition, lipid peroxidation in the microsome of rat liver is also inhibited by silymarin (Feher *et al*., 1987; Valenzuela *et al*., 1989).

The properties of silymarin that has been reported from many researches is that it can block apoptosis induced by the low doses of UVB (15-30 mJ/cm^2) in HaCaT cells. On the other hand, at a high dose of UVB, silymarin surprisingly enhanced UVB-initiated apoptosis with a strong down-regulation of AP-1 activation. Moreover, silymarin also inhibited UVB-induced proliferation of epidermal cell and sunburn or apoptotic cell formation. Some studies suggested that the protective effect of silymarin *in vivo* against UVB-induced DNA damage of epidermal is possibly by the increase of p53-Cip1/p21 resulting in the decrease in both apoptosis and cell proliferation (Agarwal *et. al*., 2006).

CHAPTER III

MATERIALS AND METHODS

In this research, cell viability in response to UVB was determined by MTT assay, and mode of cell death was confirmed using Hoechst 33342 and propidium iodide (PI) co-staining. After that, reactive oxygen species (ROS)-induced by UVB was investigated in the human keratinocyte cells model (HaCaT), and the appropriate kinetic equation was identified. Then, specific ROS probes were investigated in HaCaT cells and generated appropriate kinetic equation. HaCaT cells were pretreated with vitamin C, vitamin E, and silymarin, well-known antioxidants, prior to exposed with several doses of UVB. The ROS level and kinetic constant were investigated. Finally, the correlation of cell death and kinetic constant k value was identified the most effective factor that induces HaCaT cell death.

Materials

1. *Cells culture*

Human keratinocyte (HaCaT) cells were obtained from the Cell Lines Service (Heidelberg, Germany). HaCaT cells were cultured in Dulbecco's modified Eagle's medium, or DMEM medium (GIBCO, USA) containing 10% fetal bovine serum (FBS), 2 mM L-glutamine, and 100 units /mL penicillin/streptomycin in a 5% CO_2 environment at 37 ℃. The experiments were performed when the cells grow to 60-80% confluence, and the cells were sub-cultured at the interval times of 48 h.

2. Reagents

The vitamin C, vitamin E, silymarin, dimethysulfoxide (DMSO), ethylenediaminetetraacetic acid (EDTA), DMEM, 7'-dichlorofluorescein diacetate ($DCFH_2$-DA), 3-(4,5-Dimethylthiazol-2-yl)-2,5-diphenyltetrazolium bromide (MTT), propidium iodide (PI), and Hoechst 33342 were obtained from Sigma Chemical, Inc. (St. Louis, MO, USA). Dihydroethidium (DHE), 3'-(p-hydroxyphenyl) fluorescein (HPF), and 10-acetyl-3, 7-dihydroxyphenoxazine (Amplex Red) were obtained from Molecular Probes Inc. (Eugene, OR, USA).

Instruments

- Fluorescence microplate reader (Beckton Dickinson, Rutherford, NJ)
- Fluorescent microscope (Olympus IX51 with DP70)
- UV irradiator IL 1700 (Newburyport, Massachusetts)
- UV detector SED 007 (Newburyport, Massachusetts)

Methods

1. Sample preparation

Vitamin C was freshly prepared by diluting with PBS to obtain the desired concentrations. Vitamin E and silymarin were prepared by diluting with DMSO at the first step, then diluting with PBS to obtain the desired concentrations. The final concentration of DMSO in cell culture medium should be less than (v/v) 0.5%.

2. Ultraviolet irradiation

The aim of this study was to investigate the effect of ultraviolet B (UVB) irradiation on HaCaT cells. UVB was used as a source of ultraviolet irradiation in this study.

UV irradiator IL 1700(Newburyport, Massachusetts) was used as a source of UVB, which signal of UVB at the basement level is $1.750E^{-03}$ W/cm^2. Briefly, HaCaT cells at density of 10,000 cells per well were plated into 96-well plates in growth medium. After cell attachment, the growth medium was removed and the fresh serum free medium was immediately added. Serum free medium were removed before the cells are exposed with the several doses of UVB from (0, 40, 60, and 90 J/m^2). Non-irradiated cells were used as a control, and the results were collected in specified time intervals.

3. Cytotoxicity assay

The purpose of this study was to investigate the effect of UVB on cell viability, which examined mitochondria dehydrogenase enzyme activity. After irradiation, cells in 96-well plates were incubated with 500 μg/ml of MTT at 37° C for 4 h. The supernatant was removed and replaced with 100 μl of DMSO to dissolve the formazan crystal. The intensity of formazan product was measured at 570 nm using a microplate reader. The percent of cell viability compared with non-irradiated or non-treated control were calculated and represented as relative cell viability.

$$\text{Cell viability (\%)} = \frac{A_{570} \text{ of treatment} \times 100}{A_{570} \text{ of control}}$$

4. Apoptosis and necrosis assay

Apoptotic and necrotic cell death were determined using Hoechst 33342 and propidium iodide (PI) co-staining. After UVB exposure, cells were incubated with 10 μM of Hoechst and 5 μg/ml of PI dye for 30 m at 37°C. Condensed chromatin and/or fragmented nuclei of apoptotic and PI-positive necrotic cells were visualized under a fluorescence microscope.

5. ROS detection

Intracellular ROS was determined by using a specific fluorescent probe ($DCFH_2$-DA), superoxide anion was determined by dihydroethidium (DHE), hydroxyl radical was determined by 3'-(p-hydroxyphenyl) fluorescein (HPF), and hydrogen peroxide was determined by 10-acetyl-3, 7-dihydroxyphenoxazine (Amplex Red). After irradiation, the mixture of fresh serum free medium and specific ROS detector probe, 10 μM of $DCFH_2$-DA and HPF, 20 μM of DHE, and 10 μM of 1 X Amplex Red kit, were immediately added to the cells. After indicated times, cellular ROS signal was visualized under fluorescence microscope, and analyzed by fluorescence microplate reader (Beckton Dickinson, Rutherford, NJ) using a 488-nm excitation beam and a 530-nm band-pass filter for detecting $DCFH_2$-DA, a 490-nm excitation beam and a 515-nm band-pass filter for HPF, a 488-nm excitation beam and a 610-nm band-pass filter for DHE, a 530-nm excitation beam, and a 590-nm band-pass filter for Amplex Red. The ROS values were calculated, and compared to non-irradiation and non-treated control cells.

Experimental Design

1. Investigation on the cytotoxic effect of UVB in HaCaT cells

To investigate HaCaT cell death, cytotoxicity assay was performed in this experiment. HaCaT cells were plated at the density of 1 x 10^4 cells per well in a 96-well plate. After the cells were completely attached, the serum-containing medium was replaced with serum-free medium. The cells are exposed with the various doses of UVB (0, 40, 60, 90 J/m^2), and cell viability was analyzed by MTT assay for various time points (0, 6, 12, 24 h) after UVB exposure. Mode of cell death was determined using Hoechst 33342 and propidium iodide (PI) co-staining assay.

2. Investigation on the UVB-mediated ROS generation and kinetics in HaCaT cells

Cells were seeded at the density of 10,000 cells per well in 96 well plate and incubated in serum-free condition overnight. Then cells were exposed with three doses (0, 40, 60, 90 J/m^2) of UVB. After that, the intracellular ROS probe, $DCFH_2$-DA was added to the cell. The results were collected in the specified time intervals (0-6 h), and the results of intracellular fluorescence intensity were obtained using fluorescent microplate reader. After that, the results were used to fit the appropriate kinetic equations.

3. Identify the specific ROS and their kinetics after UVB irradiation

Briefly, cells were seeded at the density of 10,000 cells per well in 96-well plate, and incubated in serum-free condition overnight. Cells were exposed with three doses of UVB (0, 40, 60, 90 J/m^2)**,** then immediately treated with the various specific ROS probe, DHE, HPF, and Amplex Red. Fluorescence intensity was collected in the specified time intervals (0-6 h) using the fluorescence microplate reader.

In this study, the specific ROS-induced by UVB was compared and the most effective ROS generation was obtained. After that, the results were determined to fit the appropriate kinetic equations.

4. The effect of vitamin C, vitamin E, and silymarin on UVB-induced ROS generation and kinetics in HaCaT cells

Firstly, cells were seeded at the density of 1×10^4 cells per well and then incubated with various concentrations of vitamin C (0.1, 0.5, 1, 2.5, 5, 10 mM), vitamin E (0.1, 0.5, 1, 2.5, 5, 10 mM) and silymarin (0.01, 0.1, 0.5, 1, 2.5, 5 mM) for 24 h. Cells viability was determined by MTT assay, and non-toxic dose was further used in the next experiment.

The effect of known antioxidant on general ROS level was investigated in HaCaT cells using $DCFH_2$-DA as a probe. Cells were seeded at the density of 10,000 cells per well in 96-well plate, and incubated in serum-free condition overnight. Next, HaCaT cells were pretreated with non-toxic concentrations of vitamin C (0.1, 0.5, 1 mM), vitamin E (0.1, 0.5, 1 mM), and silymarin (0.01, 0.1, 0.5 mM), then incubated at 37°C for 1 h. After that, cells were exposed with various doses of UVB **(**0, 40, 60, 90 J/m^2). The intracellular ROS was investigated by $DCFH_2$-DA at the different times (0-6 h). After that, the appropriate kinetic equations were generated.

5. Investigation on the correlation between the kinetic constant value and cell death effect.

Cells were seeded at the density of 10,000 cells per well in 96-well plate and incubated in serum-free condition overnight. After cells were exposed with UVB, the results were obtained, and identified for the appropriate kinetic equations in order to obtained the kinetic constant value. The kinetic constants values of non-irradiation

and UVB-irradiation were used to plot the correlation graph with percentage of cell viability and apoptosis.

6. Statistical Analysis

Data are demonstrated as the means ± S.D. from three or more independent experiments. Statistical analysis was performed using one-way ANOVA and post hoc test (Dunnett's test). A P-value of less than 0.05 would be considered as statistically significant. Correlation analysis will be performed by SPSS program version 17.

CHAPTER IV

RESULTS

1. Investigation of the cytotoxic effect of UVB in HaCaT cells

Cytotoxic effect of UVB was first observed in term of cell viability, apoptosis and necrosis assays. Human keratinocytes were seeded in 96-well plate and then incubated in the serum free condition overnight. Cells were exposed with the various doses of UVB (0, 40, 60, and 90 J/m^2) for 0-24 h. Cell viability and cell death (apoptosis and necrosis) were measured.

The results demonstrated that viability of the cells exposed to UVB at 40, 60, and 90 J/m^2 for 6 h were significantly decreased as compared to that of non-treated cells (0 J/m^2). Cell viability was continuously decreased up to 24 h in a time-dependent manner which cell viability was remained 50% after irradiation with 90 J/m^2 UVB for 24 h as shown in figure 4.1A. For the nuclear morphology study, apoptosis cell death was significantly detected at 6 h in response to 40, 60, and 90 J/m^2 of UVB, respectively (Figure 4.1B), while propidium iodide (PI) stained cells were observed after UVB exposure for 12 h, indicating late apoptosis as shown in figure 4.1C. These results suggested that UVB-induced apoptosis in HaCaT was observed as early as 6 h, corresponding with the decrease in cell viability.

A.

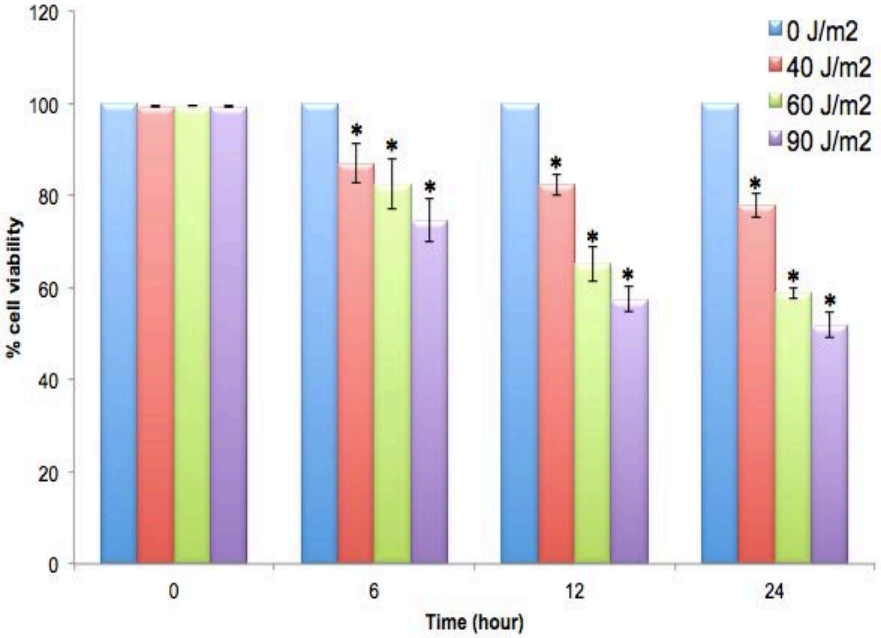
120
100
80
60
40
20
0
% cell viability
0 J/m2
40 J/m2
60 J/m2
90 J/m2
0
6
12
24
Time (hour)

B.

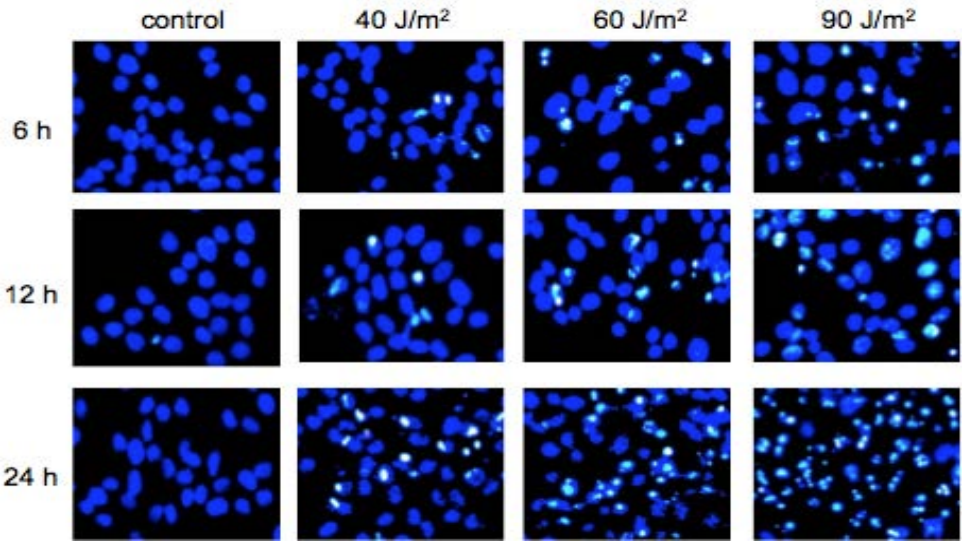
control
40 J/m²
60 J/m²
90 J/m²
6 h
12 h
24 h

C.

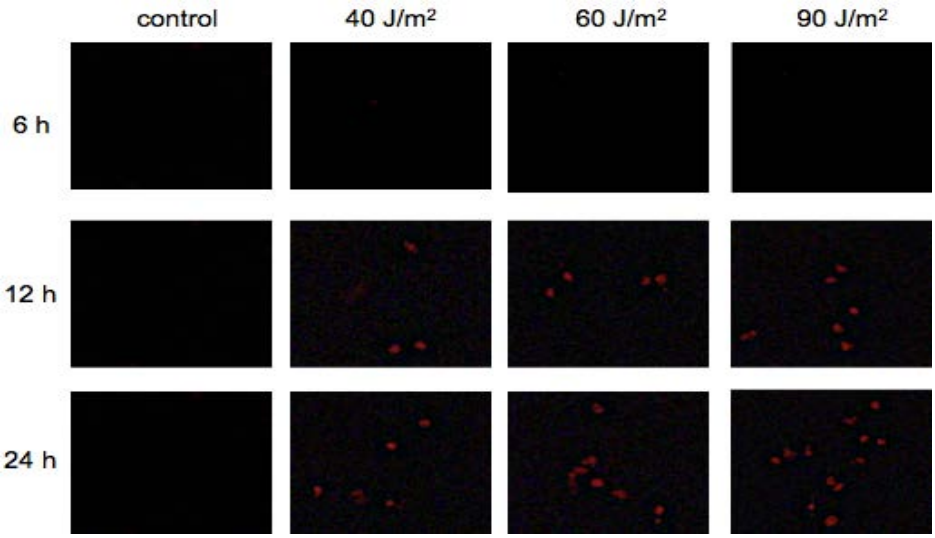

Figure 4.1 Effect of UVB on HaCaT cells. A) Cells were exposed with several doses of UVB (0, 40, 60, 90 J/m^2) for 0, 6, 12, and 24 h, and cell viability was measured by MTT assay. B) Nuclear morphology of apoptosis cells was detected using Hoechst 33342. C) Nuclear morphology of late apoptosis cells was detected using PI assays. Values represented the mean ± S.D. (*n = 4*) *, P < 0.05 versus non-treated control cells.

2. Investigation of the UVB-mediated ROS generation and kinetics in HaCaT cells

2.1 UVB-induced the intracellular ROS production in HaCaT cells

To investigate the effect of UVB on oxidative status of human keratinocytes (HaCaT), cells were exposed to several doses of UVB (0, 40, 60, and 90 J/m^2) and the intracellular ROS signals were evaluated using $DCFH_2$-DA probe at 0-6 h. Figure 4.2A shows a time-dependent accumulative ROS signal in the cells. Importantly, UVB irradiation caused an extreme increase in the rate of intracellular ROS accumulation in a dose-dependent manner. In response to UVB irritation, the induction of ROS signal was significantly detected as early as 1 h after exposure and such an increase of oxidative stress in keratinocytes was found to be in a dose-dependent manner up to 90 J/m^2 of UVB. Also, the ROS signal representing by an increase of intracellular DCF fluorescence signal was demonstrated in figure 4.2B.

A.

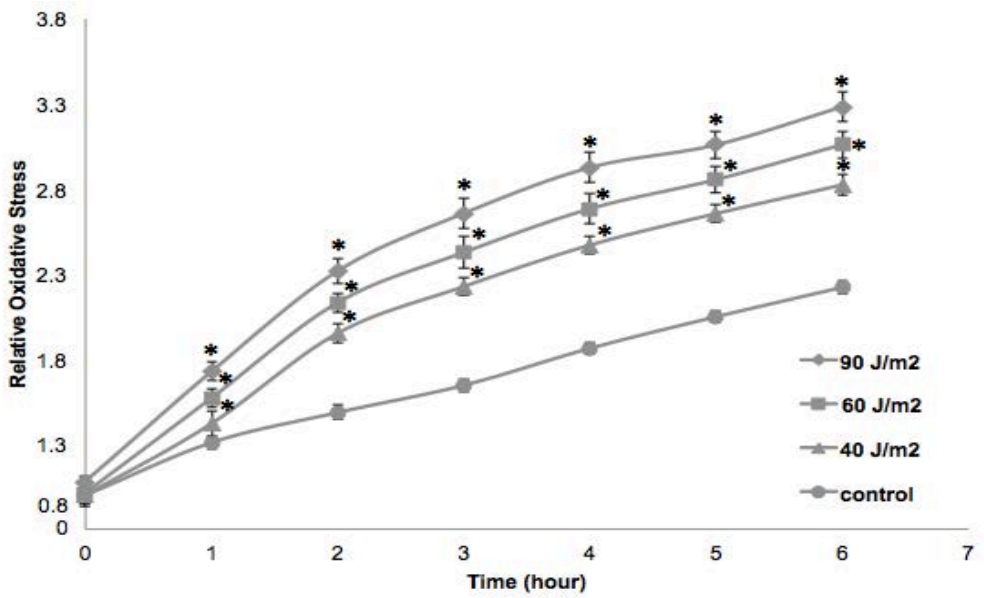

B.

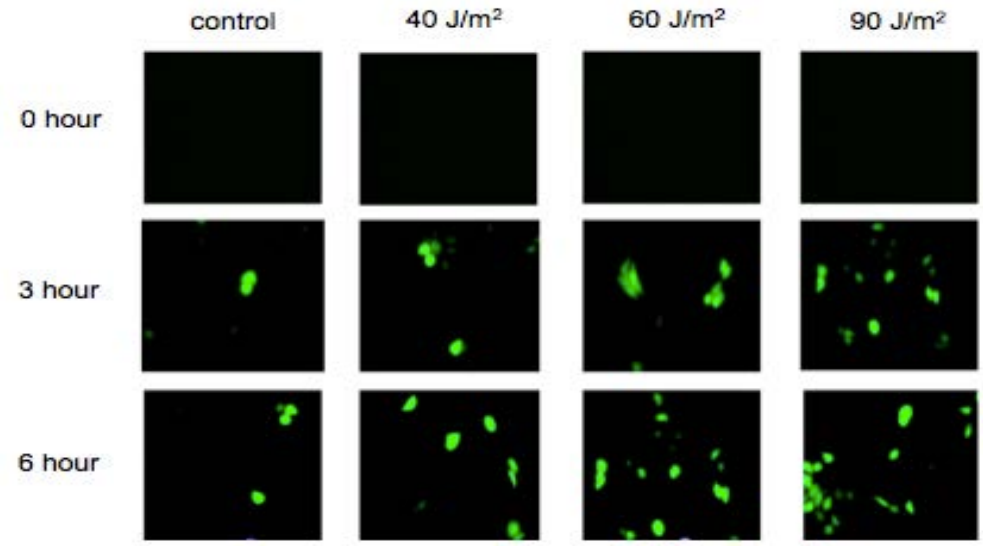

Figure 4.2 UVB induced intracellular ROS generation in keratinocytes. A) Cells were exposed to various doses of UVB (0-90 J/m^2) for 0-6 h, and intracellular ROS was detected by $DCFH_2$-DA probe using fluorescence microplate reader. Data point represent the mean ± S.D. (*n = 4*) *, P < 0.05 versus non-irradiation control cells at the same time point. B) Cellular ROS signal were determined by $DCFH_2$-DA fluorescence measurements.

2.2 The Kinetics of intracellular ROS in response to UVB in HaCaT cells

It was very interesting that the rate of ROS production in the UVB-treated cells appeared to be accelerated in the first 2 h period in comparison to that of control cells and then rate decreased to the level of basal ROS generation after 2-6 h. These kinetics data suggested that UVB mediated intracellular oxidative stress in an early phase (~2 h) after an exposure to the UVB. The 2 distinct phases of ROS production were evaluated and found that the pattern of ROS induction rate was fitted to the linear trend line in both phases. The R^2 were more than 0.97 was accepted as shown in Figure 4.3A and B. The rate constant (k) of each UVB dose was then verified by linear equation as $y = k_0t + y_0$. Figure 4.3A demonstrated that 90 J/m^2 of UVB exhibited the highest k value which was 0.6376, compared to that of 60, 40, and 0 J/m^2 which were 0.5484, 0.5054, and 0.2695, respectively. Next, the difference of ROS production rate in these cells seems to be minimal at the time of 2-6 h as shown in figure 4.3B. These data suggested that the oxidative stress in keratinocyte in response to UVB exposure was mainly caused by the induction of cellular ROS with in 2 h after irritation.

A.

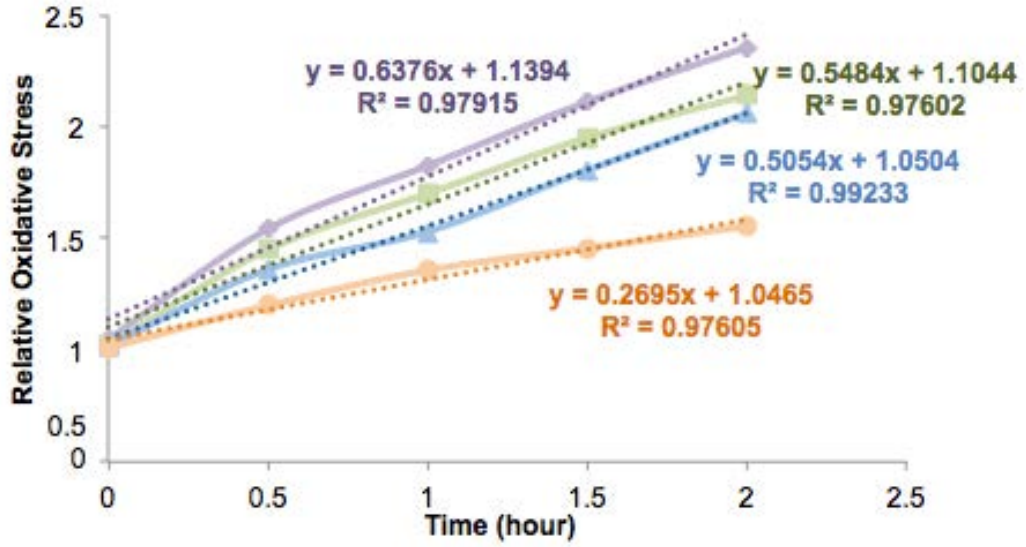

B.

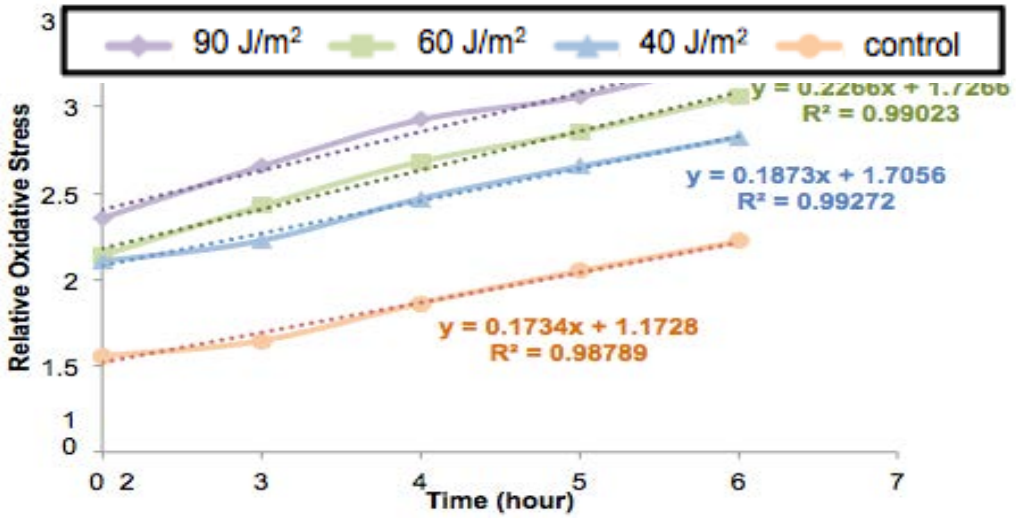

Figure 4.3 Kinetics of intracellular ROS production. A) Kinetics of intracellular ROS in response to UVB (0-90 J/m^2) at 0-2 h after UVB irradiation. B) Kinetics of intracellular ROS in response to UVB (0-90 J/m^2) at 2-6 h after UVB irradiation. Accumulative intracellular ROS content was evaluated by fluorescence microplate reader, *n = 4*.

3. Identify the specific ROS and their kinetics after UVB irradiation

3.1 The specific ROS induced by UVB irradiation

The specific probes as DHE, Amplex Red, and HPF were used in this experiment in order to detect the specific ROS generated after UVB exposure. HaCaT cells were seeded in a 96-well plate and incubated in a serum-free medium over night before exposed to several doses of UVB (0-90 J/m^2). The specific probes were added after cells were exposed and the results of fluorescence intensity were collected in the time-dependent manner from 0-6 h. Figure 4.4 reveals that superoxide anion, hydrogen peroxide, and hydroxyl radical increased in response to UVB in time and dose-dependent manners.

However, the rate of each ROS production was significantly distinguishable. Figure 4.4A shows that HPF signal indicating hydroxyl radical level was found to increase as early as 15 min after UVB irradiation and the rate of hydroxyl radical increase was significantly higher in the UVB-treated cells over control in the early phase (0-1 h). Also, Amplex Red data demonstrated that H_2O_2 was gradually generated in the cells in time-dependent manner and the effect of UVB on H_2O_2 production could be detected only after 2 h of UVB exposure as shown in figure 4.4B. However, DHE intensity representing superoxide anion ($^{\bullet}O_2^-$) level indicated that the dramatic increase of superoxide anion in response to UVB was observed in the early 2 h after UVB exposure as shown in figure 4.4C. The superoxide signal representing by an increase of DHE fluorescence signal was confirmed in figure 4.4D.

It is worthy to note herein that superoxide anion and hydroxyl radical were found to be specific ROS affected by an UVB exposure in the early phase and superoxide anion which was the most affected one with approximately 2.5-fold induction could be detected in response to 90 J/m^2 of UVB. Thus, superoxide anion and hydroxyl

radical could be the principal specific ROS produced in keratinocytes and responsible for the oxidative stress mediated by UVB irradiation.

A.

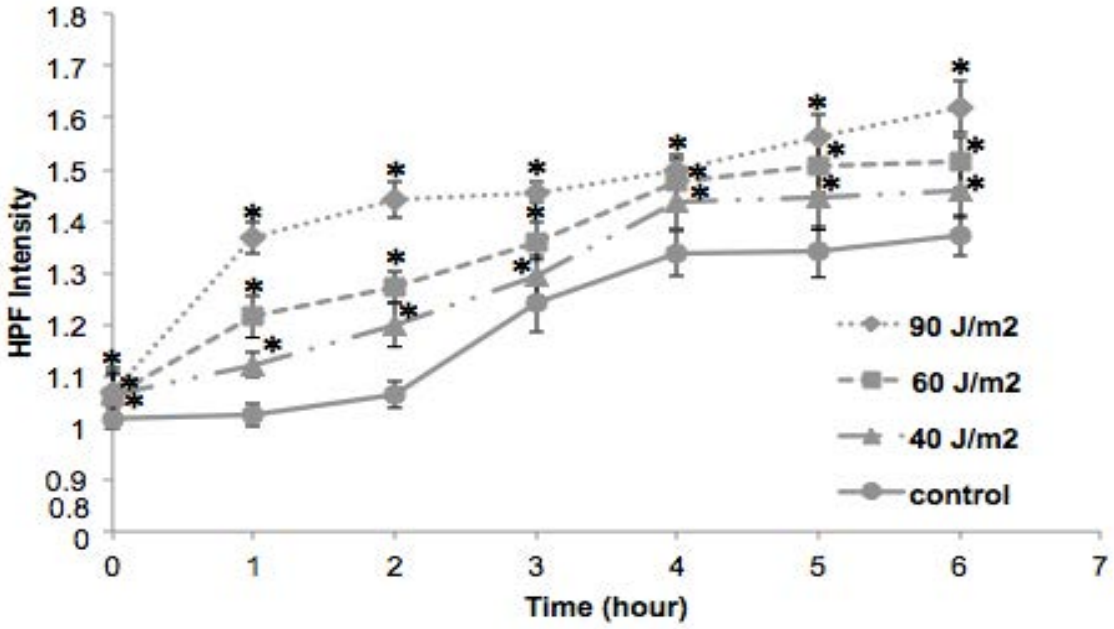

B.

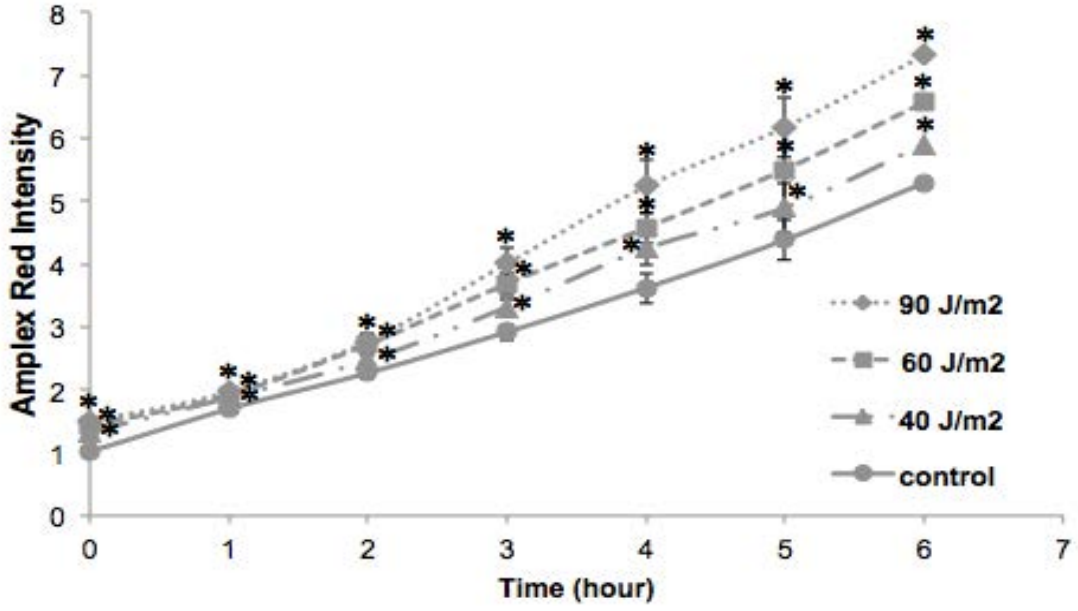

C.

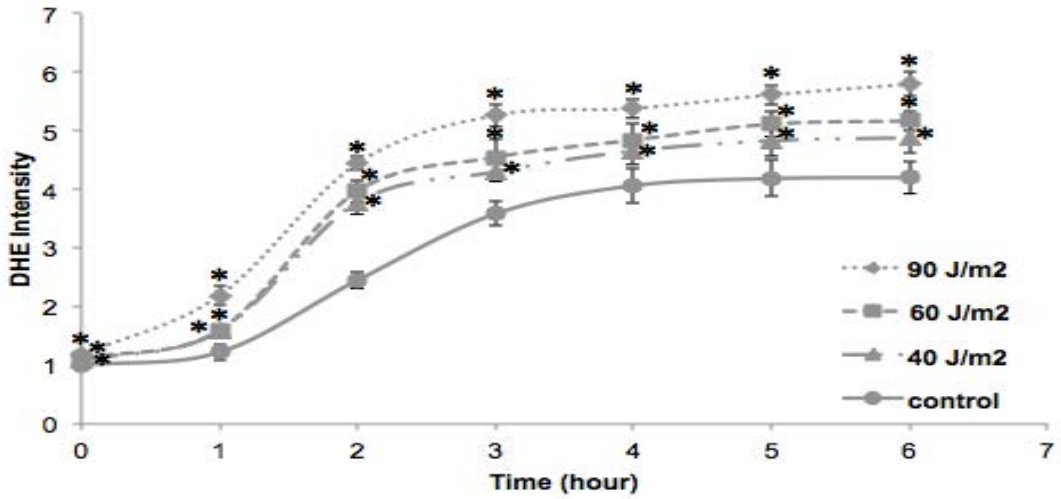

D.

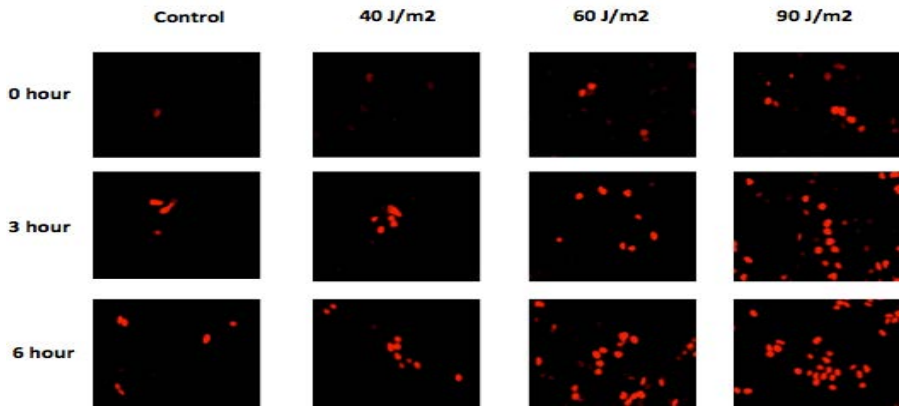

Figure 4.4 Identification of specific ROS generation in response to UVB irradiation. Cells were exposed to various doses of UVB and accumulation of specific ROS was determined by specific ROS probes. A) HPF probe was used for the detection of hydroxyl radical accumulation. B) Amplex Red was used as a specific probe to detect hydrogen peroxide level. C) DHE fluorescence probe was used for the detection of superoxide anion level. Data point represent the mean ± S.D. (*n = 4*) *, P < 0.05 versus non-treated control cells at the same time point. D) Superoxide anion induction in HaCaT were stained with DHE and visualized under fluorescence microscope.

3.2 The kinetics of specific ROS production mediated by UVB

Using the data of 90 J/m^2 UVB, the plots representing each specific ROS generation were generated. Figure 4.5 demonstrated the graph plotting signals of DHE, Amplex Red, and HPF in the keratinocytes exposure to UVB against time. The results revealed that DHE induction was fitted to the polynomial trend line with the k value = 0.3993 and R^2 = 0.9955 (Figure 4.5C). Amplex Red induction was aligned with the exponential equation to obtain the k value of 0.3109 and the R^2 = 0.99344 (Figure 4.5B), while the rate of HPF increase fitted with linear equation exhibited the lowest k value = 0.1697 and the R^2 = 0.98706 as shown in figure 4.5A. This information led to the understanding that specific ROS generated in response to UVB exposure in human keratinocytes was found to be in the different kinetics.

A.

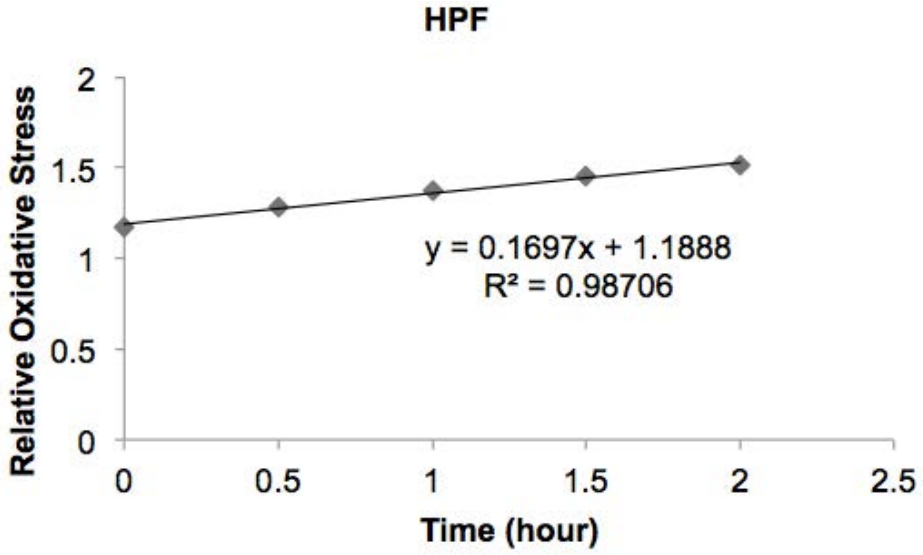

B.

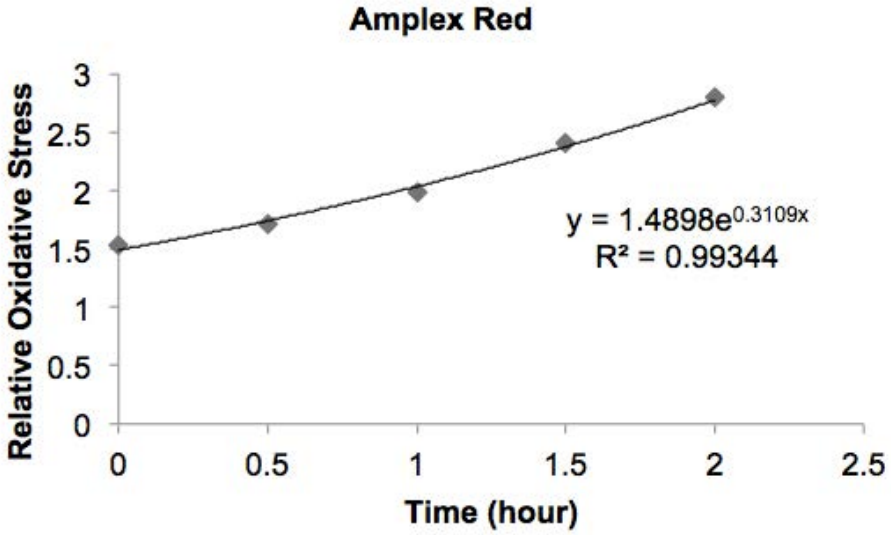

C.

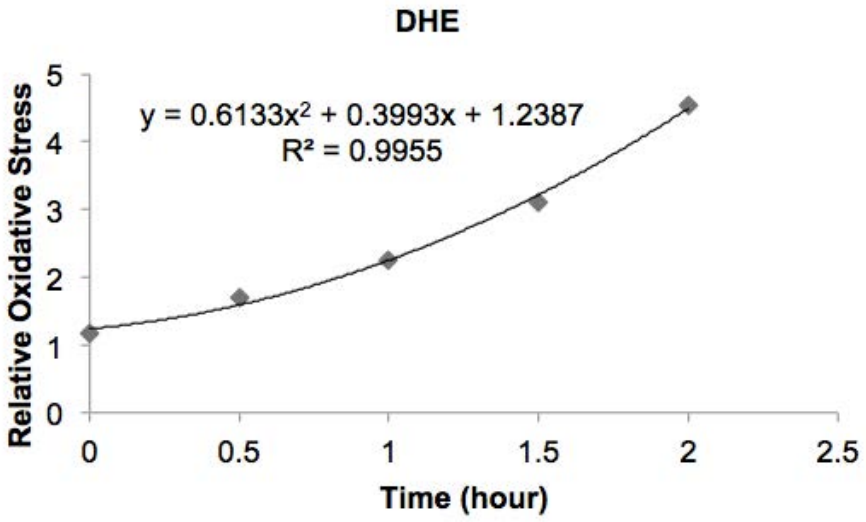

Figure 4.5 Kinetics of specific ROS generated in response to UVB irradiation. A) Kinetics of hydroxyl radical in response to 90 J/m^2 UVB was determined using HPF as specific probe. B) Kinetics of hydrogen peroxide in response to 90 J/m^2 UVB was determined using Amplex Red as specific probe. C) Kinetics of superoxide anion in response to 90 J/m^2 UVB was determined using DHE as specific probe. Data points represent the mean ± S.D. (*n = 4*).

4. The effect of vitamin C, vitamin E, and silymarin on UVB induced ROS generation and kinetics in HaCaT cells.

4.1 Effect of vitamin C on HaCaT cells.

4.1.1 Effect of vitamin C on cell viability in HaCaT cells.

To investigate the cytotoxicity effect of vitamin C, HaCaT cells were treated with vitamin C at the concentrations of 0.1, 0.5, 1, 2.5, 5, 10 mM, and cell viability was examined by MTT assay.

The result suggested clearly that cell viability was decreased on response to vitamin C treatment in dose-dependent manner. After treatment for 24 h, cell viability was significantly decreased to 66.78 ± 4.21, 52.00 ± 2.25, and 40.56 ± 1.08 in cells treated with 2.5, 5, and 10 mM of vitamin C, respectively (figure 4.6), where as no significant change were observed in cells treated with 0.1-1 mM of vitamin C.

These results suggested that the low doses of vitamin C (0.1-1 mM) were non-toxic to cells. These concentrations therefore would be used in further experiment to investigate whether UVB was able to induced ROS generation in HaCaT under the presence of vitamin C.

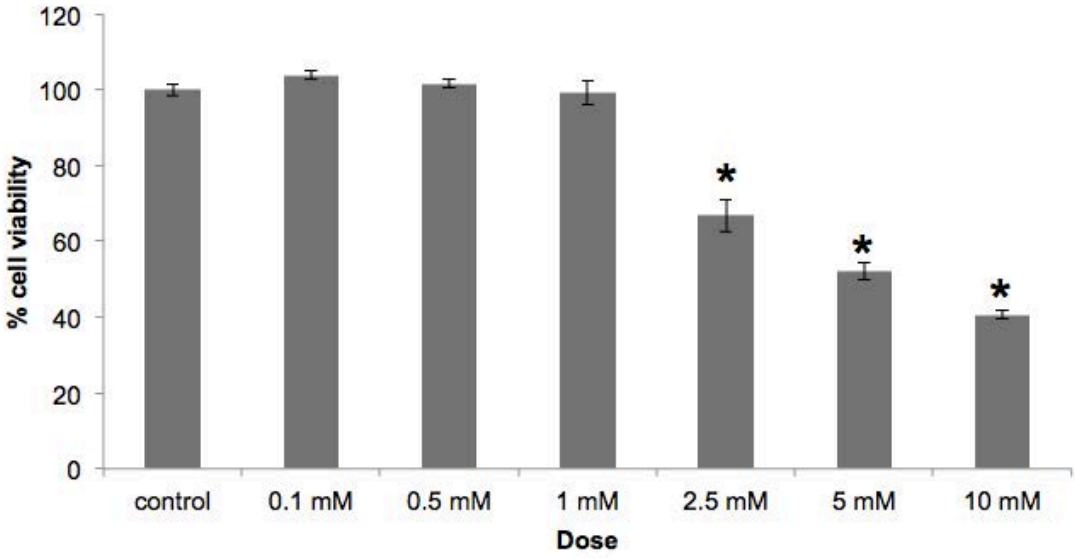

Figure 4.6 Cytotoxicity of vitamin C on HaCaT. Cells were treated with various concentrations of vitamin C (0.1, 0.5, 1, 2.5, 5, and 10 mM) for 24 h. Cell viability was determined by MTT assay. Values represent the mean ± S.D. (*n = 4*) *, P < 0.05 versus non-treated control cells.

4.1.2 Effect of vitamin C on ROS production-induced by UVB in HaCaT cells.

In order to investigate the effect of vitamin C on ROS production-induced by UVB, HaCaT were pretreated with vitamin C for 1 hour prior to UVB irradiation (0, 40, 60, and 90 J/m^2). After an UVB exposure, intracellular ROS was detected using ROS detection probe, $DCFH_2$-DA and analyzed by fluorescence microplate reader as described. The non-toxic concentrations of vitamin C (0.1, 0.5, and 1 mM) were used in this experiment.

The results indicated that the elevation of ROS in response to UVB exposure as shown in figure 4.2A could be protected by pretreatment of vitamin C. In response to UVB irradiation in vitamin C treated cells (0.1, 0.5, and 1 mM), the induction of ROS signal still caused significant increased in accumulated ROS level in a dose-dependent manner. The irradiation of 90 J/m^2 of UVB had shown the highest ROS signal followed by 60, 40, and 0 J/m^2 (Figure 4.7).

Figure 4.8A confirmed that the protective effect of vitamin C on oxidative status in cells exposed with 90 J/m^2 of UVB compared to non-treated cells. Vitamin C (0.1, 0.5, and 1 mM) caused a significant decrease in UVB-induced ROS generation in dose-dependent manner as compared to non-treated cells. The alteration of ROS generating rate could be detected during 0 to 6 h after an UVB exposure in the present of 1 and 0.5 mM vitamin C. In contrast, 0.1 mM of vitamin C only slightly decreased ROS level during at 3 to 6 h after UVB exposure as compared to control cells. The results were confirmed by fluorescence microscope as shown in figure 4.8B, suggesting that non-toxic doses

of vitamin C suppress ROS-induced by UVB exposure as compared to non-treated cells in a concentration-dependent manner.

A.

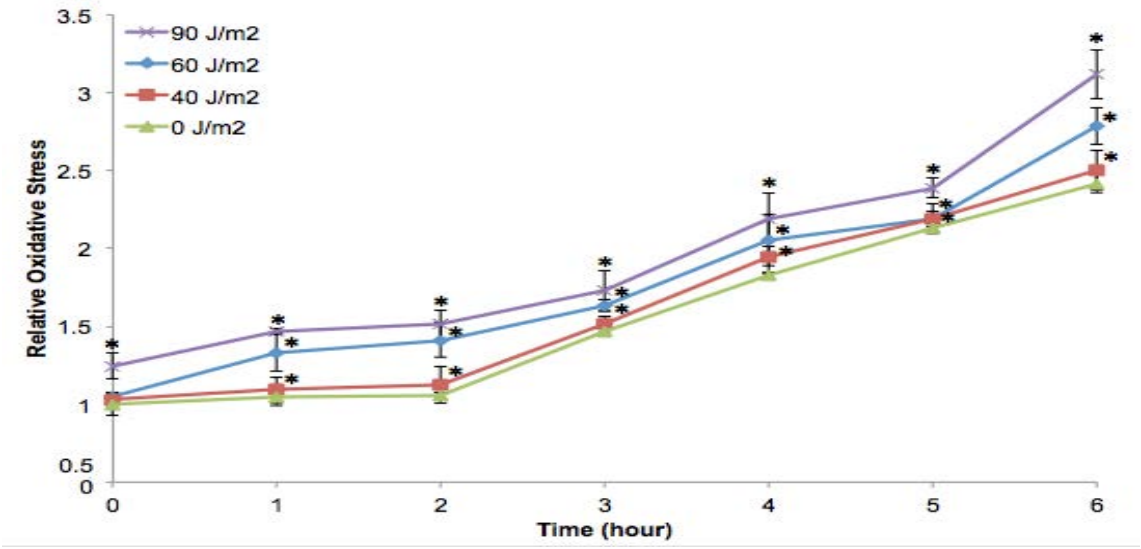

B.

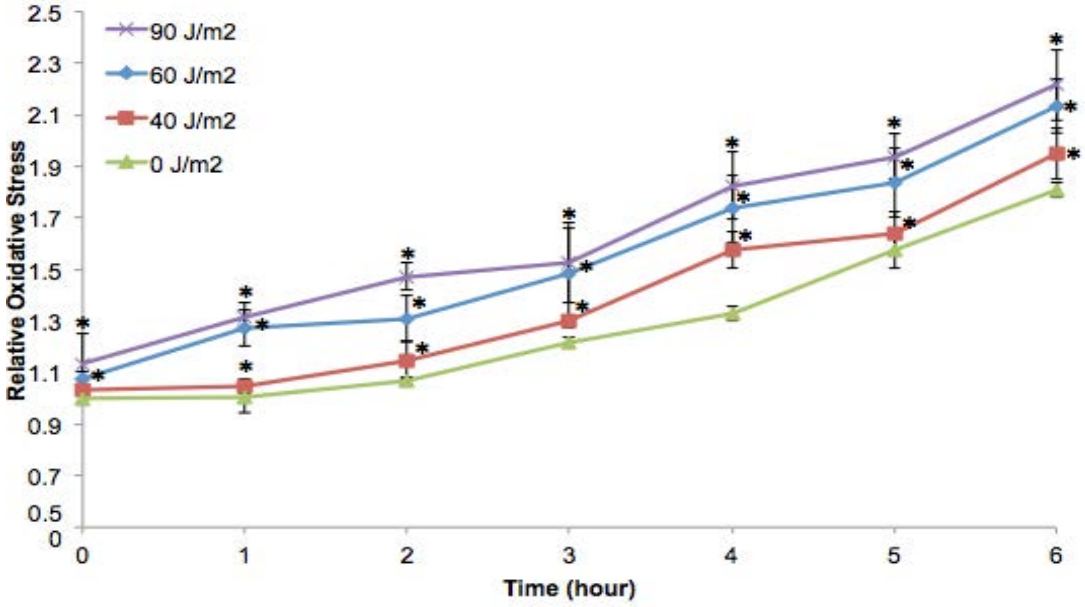

C.

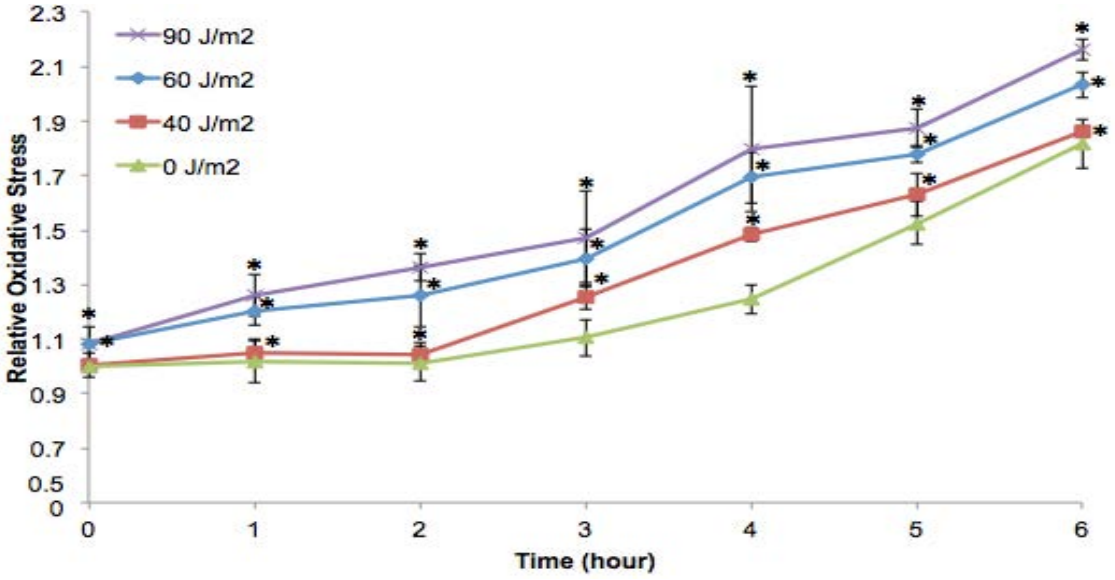

Figure 4.7 Effect of vitamin C on accumulated intracellular ROS generated by UVB. Cells were pretreated with A) 0.1 mM, B) 0.5 mM, C) 1 mM of vitamin C prior to UVB exposure. ROS generation was detected by $DCFH_2$-DA. Data point represent the mean ± S.D. (*n = 4*) *, P < 0.05 versus non-irradiation cells at the same time point.

A.

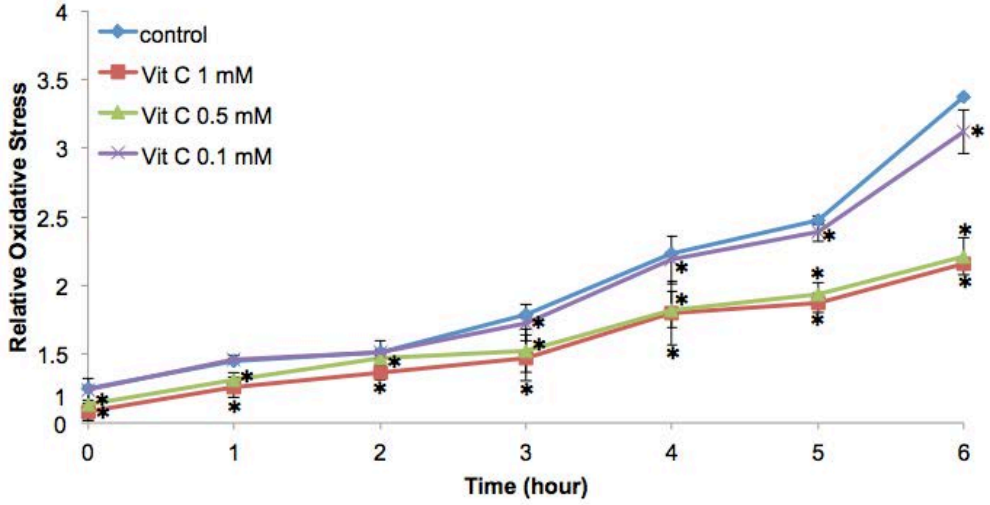

B.

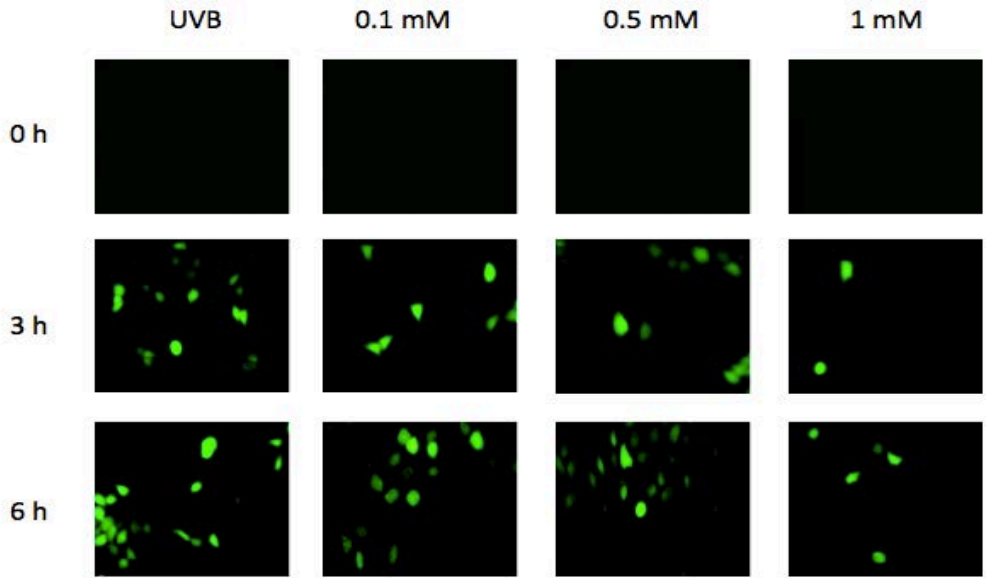

Figure 4.8 Effect of various concentrations of vitamin C on ROS production. Cells were treated with 0.1, 0.5, and 1 mM of vitamin C for 1 h prior to 90 J/m^2 UVB irradiation. A) ROS level was determined by $DCFH_2$-DA probe using fluorescence microplate reader. Data point represent the mean ± S.D. (*n = 4*) *, $P < 0.05$ versus non-treated cells at the same time point. B) Cellular ROS signal were visualized under fluorescence microscope using ROS detection probe, $DCFH_2$-DA.

4.2 Effect of vitamin E on HaCaT cells.

4.2.1 Cytotoxicity effect of vitamin E in HaCaT cells.

To investigate the cytotoxicity effect of vitamin E, HaCaT cells were treated with vitamin E at various concentrations of 0.1, 0.5, 1, 2.5, 5, 10 mM, and cell viability was examined by MTT assay.

The results indicated that cell viability was decreased in response to vitamin E treatment in dose-dependent manner. After treatment for 24 h, cell viability was significant decreased to 80.91 ± 1.15, 75.43 ± 1.02, 70.90 ± 0.94 in cells treated with 2.5, 5, and 10 mM of vitamin E, respectively (figure 4.9), whereas no significant change was observed in cells treated with 0.1-1 mM of vitamin E.

These results suggested that the low doses of vitamin E (0.1-1 mM) were non-toxic to cells. These concentrations would be therefore used in further experiment to investigate whether UVB was able to induced ROS generation in HaCaT in presence of vitamin E.

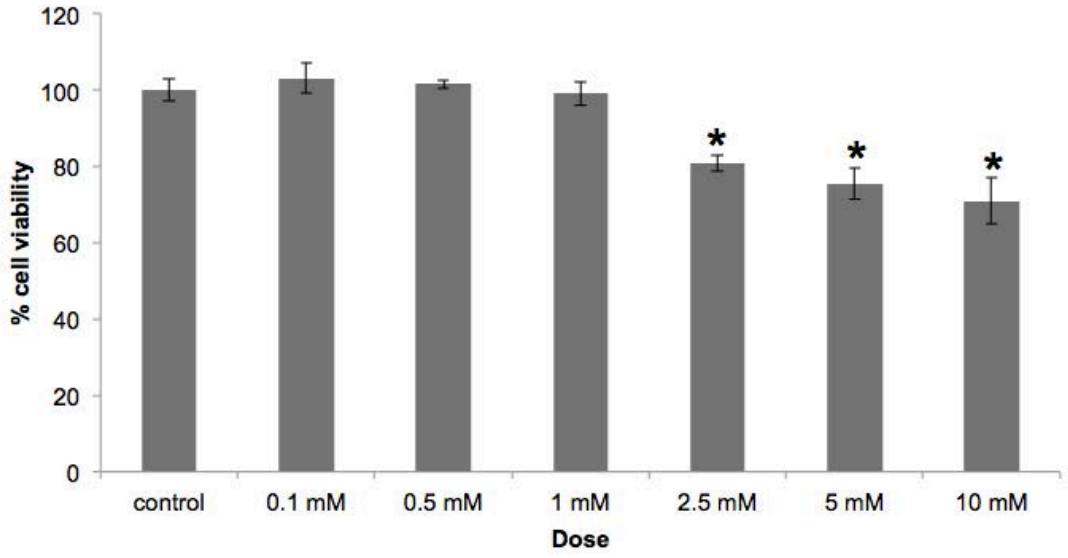

Figure 4.9 Cytotoxicity of vitamin E on HaCaT. Cells were treated with various concentrations of vitamin E (0.1, 0.5, 1, 2.5, 5, and 10 mM) for 24 h. Cell viability was measured by MTT assay. Values represent the mean ± S.D. (*n* = *4*) *, P < 0.05 versus non-treated control cells.

4.2.2 Effect of vitamin E on ROS production-induced by UVB in HaCaT cells.

In order to investigate the effect of vitamin E on ROS production-induced by UVB, HaCaT cells were incubated with vitamin E for 1 hour prior to UVB irradiation (0, 40, 60, and 90 J/m^2). After an UVB exposure, intracellular ROS was detected using ROS detection probe, $DCFH_2$-DA and analyzed by fluorescence microplate reader as described. Only non-toxic concentrations of vitamin E (0.1, 0.5, and 1 mM) were used in this experiment.

The results indicated that the elevation of ROS in response to UVB exposure as shown in figure 4.2A could be protected by pretreatment of vitamin E. In response to UVB irradiation in vitamin E treated cells (0.1, 0.5, and 1 mM), the induction of ROS signal still caused significant increased in accumulated ROS level in a dose-dependent manner. The irradiation of 90 J/m^2 of UVB had shown the highest ROS signal followed by 60, 40, and 0 J/m^2 (Figure 4.10).

Figure 4.11A confirmed the protective effect of vitamin E on oxidative stress in cells exposed with 90 J/m^2 of UVB compared to non-treated cells. Vitamin E (0.1, 0.5, and 1 mM) caused a significant decrease in ROS-induced by UVB in dose-dependent manner as compared to non-treated cells. The alteration of ROS generating rate could be detected during 0 to 6 h after an UVB exposure in the present of 1 and 0.5 mM vitamin E. In contrast, 0.1 mM vitamin E only slightly decreased in accumulated ROS level during 2 to 6 h after UVB exposure as compared to control cells. The results were confirmed by fluorescence microscope as shown in figure 4.11B, suggesting that non-toxic

doses of vitamin E suppress ROS-induced by UVB exposure as compared to non-treated cells in a concentration-dependent manner.

A.

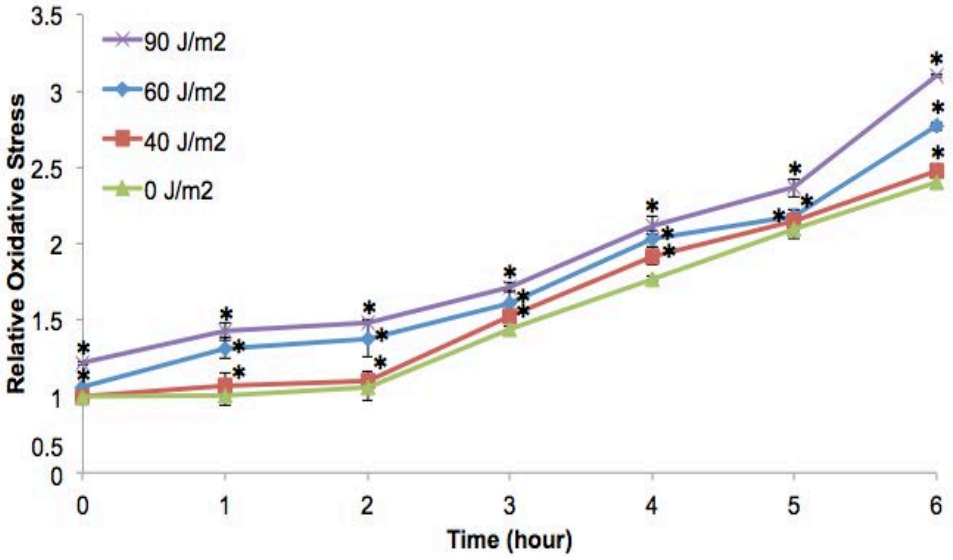

B.

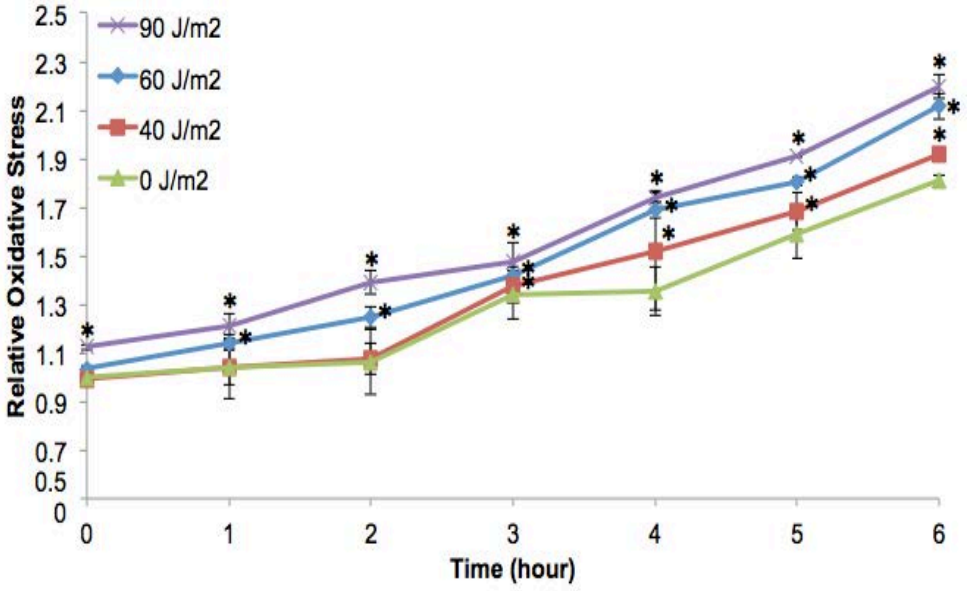

C.

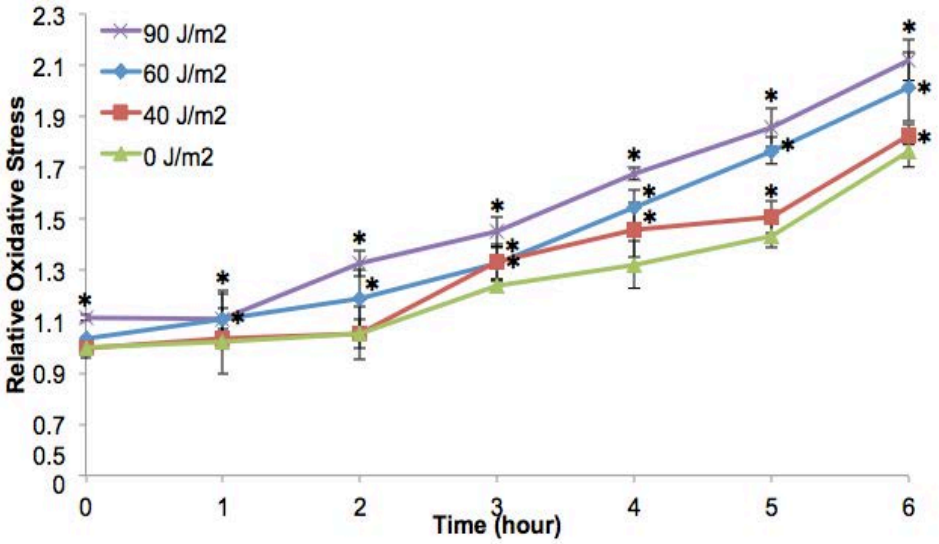

Figure 4.10 Effect of vitamin E on accumulated intracellular ROS generated by UVB. Cells were pretreated with A) 0.1 mM, B) 0.5 mM, C) 1 mM of vitamin E prior to UVB exposure. ROS generation was detected by $DCFH_2$-DA. Data point represent the mean ± S.D. (*n = 4*) *, P < 0.05 versus non-irradiation cells at the same time point.

A.

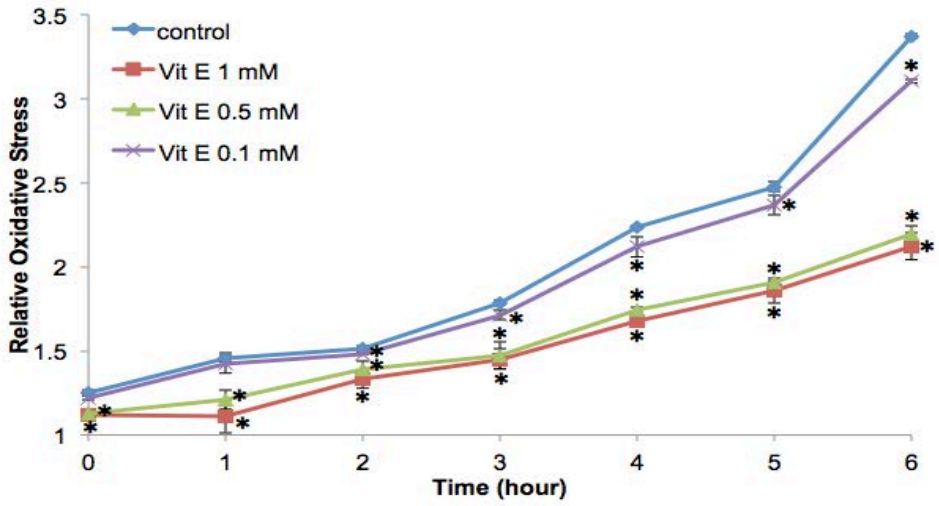

B.

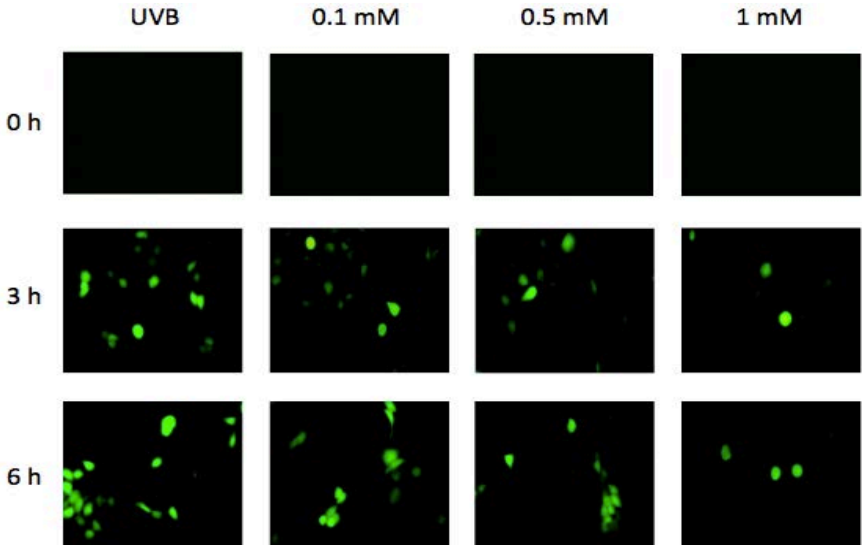

Figure 4.11 Effect of various concentrations of vitamin E on ROS production. Cells were pretreated with 0.1, 0.5, and 1 mM of vitamin E for 1 h prior to 90 J/m^2 UVB irradiation. A) ROS level was determined by $DCFH_2$-DA probe using fluorescence microplate reader. Data point represent the mean ± S.D. (*n = 4*) *, P < 0.05 versus non-treated cells at the same time point. B) Cellular ROS signal were visualized under fluorescence microscope using ROS detection probe, $DCFH_2$-DA.

4.3 Effect of silymarin on HaCaT cells.

4.3.1 Cytotoxicity effect of silymarin in HaCaT cells.

To investigate the cytotoxicity effect of silymarin, HaCaT cells, cells were treated with various concentrations of silymarin (0.01, 0.1, 0.5, 1, 2.5, and 5 mM) and cell viability was examined by MTT assay.

The results clearly indicated that cell viability was decreased in response to silymarin treatment in dose-dependent manner. After treatment for 24 h, cell viability was significantly decreased to 74.29 ± 0.01, 52.43 ± 0.01, 24.53 ± 0.08 in cells treatment with 1, 2.5, and 5 mM of silymarin, respectively (figure 4.12), whereas no significant change was observed in cells treatment with 0.01-0.5 mM of silymarin.

These results suggested that the low doses of silymarin (0.01-0.5 mM) were non-toxic to cells. These concentrations therefore would be used in further experiment to investigate whether UVB was able to induced ROS generation in HaCaT under the presence of silymarin.

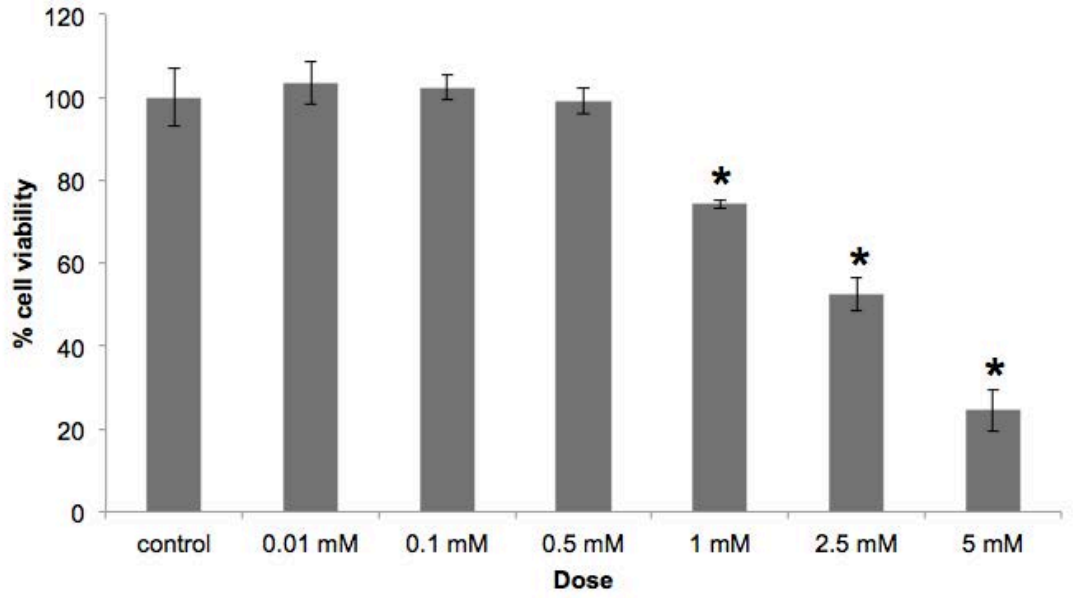

Figure 4.12 Cytotoxicity of silymarin on HaCaT. Cells were treated with various concentrations of silymarin (0.01, 0.1, 0.5, 1, 2.5, and 5 mM) for 24 h. Cell viability was determined by MTT assay. Values represent the mean ± S.D. (*n* = *4*) *, P < 0.05 versus non-treated control cells.

4.3.2 Effect of silymarin on ROS production-induced by UVB in HaCaT cells.

In order to investigate the effect of silymarin on ROS production-induced by UVB, HaCaT cells were incubated with silymarin for 1 hour prior to UVB irradiation (0, 40, 60, and 90 J/m^2). After an UVB exposure, intracellular ROS was detected using ROS detection probe, $DCFH_2$-DA and analyzed by fluorescence microplate reader as described. Only the non-toxic concentrations of silymarin (0.01, 0.1, and 0.5 mM) were used in this experiment.

The results indicated that the elevation of ROS in response to UVB exposure as shown in figure 4.2A could be protected by pretreatment of silymarin. In response to UVB irradiation in silymarin treated cells (0.01, 0.1, and 0.5 mM), the induction of ROS signal still caused significant increased in accumulated ROS level in a dose-dependent manner. The irradiation of 90 J/m^2 of UVB had shown the highest ROS signal followed by 60, 40, and 0 J/m^2 (Figure 4.13).

Figure 4.14A confirmed the protective effect of silymarin on oxidative status in cells exposed with 90 J/m^2 of UVB compared to non-treated cells. Silymarin (0.01, 0.1, and 0.5 mM) caused a significant decrease in ROS-induced by UVB in dose-dependent manner as compared to non-treated cells. The alteration of ROS generating rate could be detected during 0 to 6 h after an UVB exposure in the present of 0.5 and 0.1 mM of silymarin, while 0.01 mM of silymarin only slightly decreased in ROS level only at 6 h after UVB exposure as compared to control cells. The results were confirmed by fluorescence microscope shown in figure 4.14B, suggesting that non-toxic doses of silymarin

suppress ROS production induced by UVB exposure as compared to non-treated cells in a concentration-dependent manner.

A.

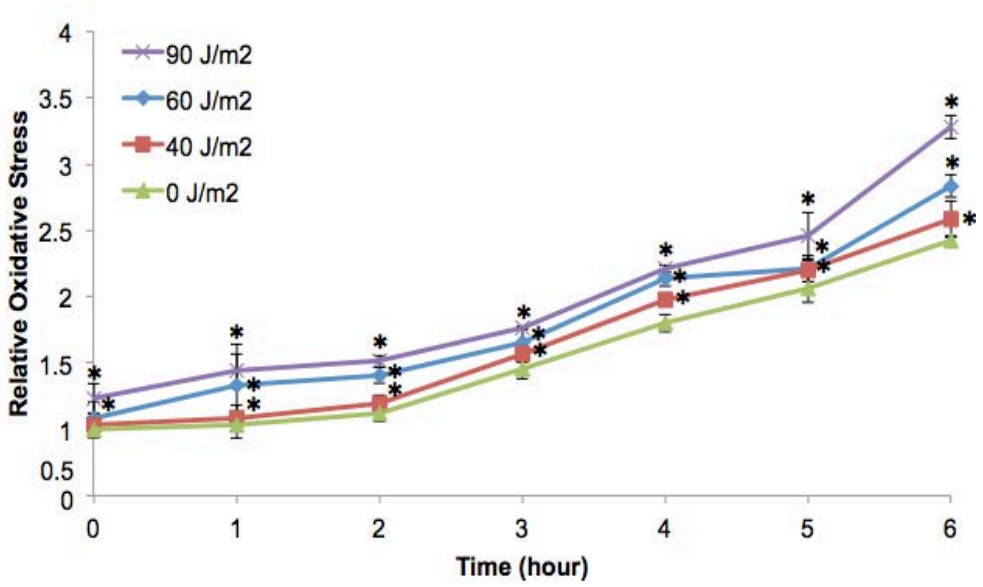

B.

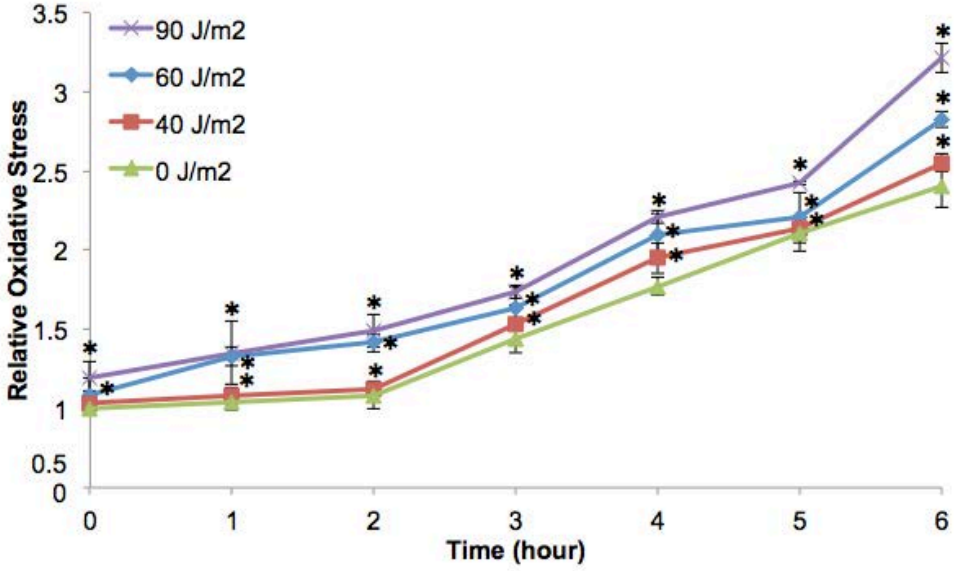

C.

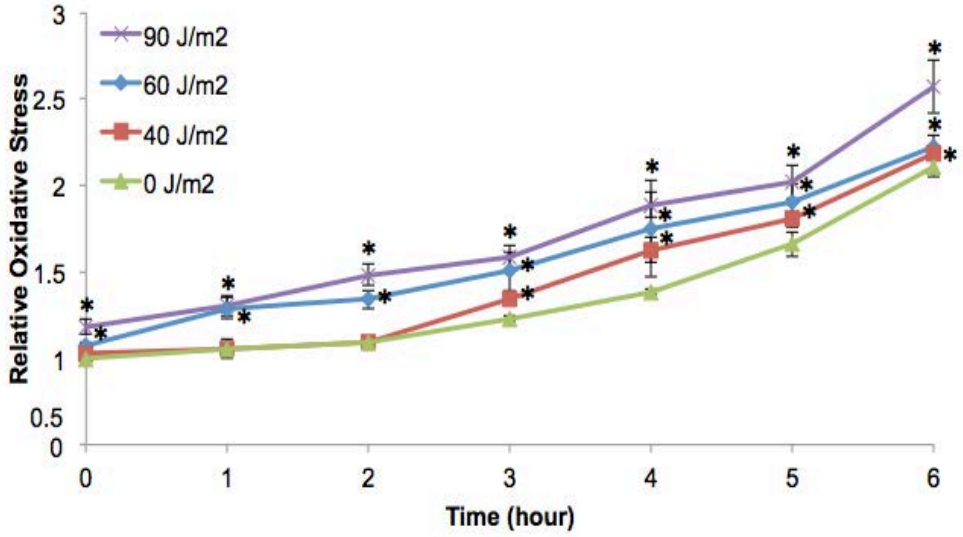

Figure 4.13 Effect of silymarin on accumulated intracellular ROS generated by UVB. Cells were pretreated with A) 0.01 mM, B) 0.1 mM, C) 0.5 mM of silymarin prior to UVB exposure, ROS generation was detected by $DCFH_2$-DA. Data point represent the mean ± S.D. (*n = 4*) *, P < 0.05 versus non-irradiation cells at the same time point.

A.

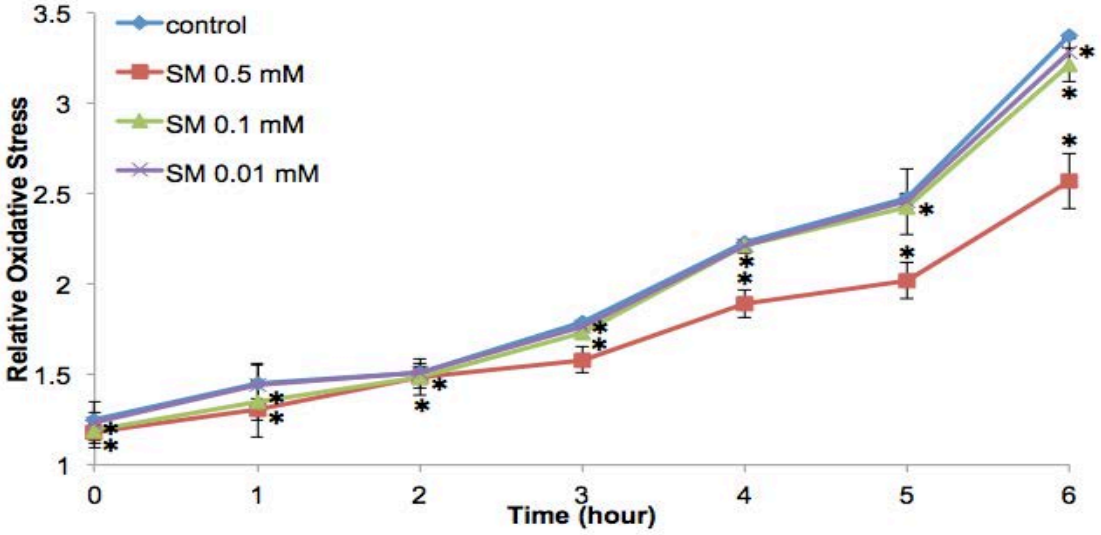

B.

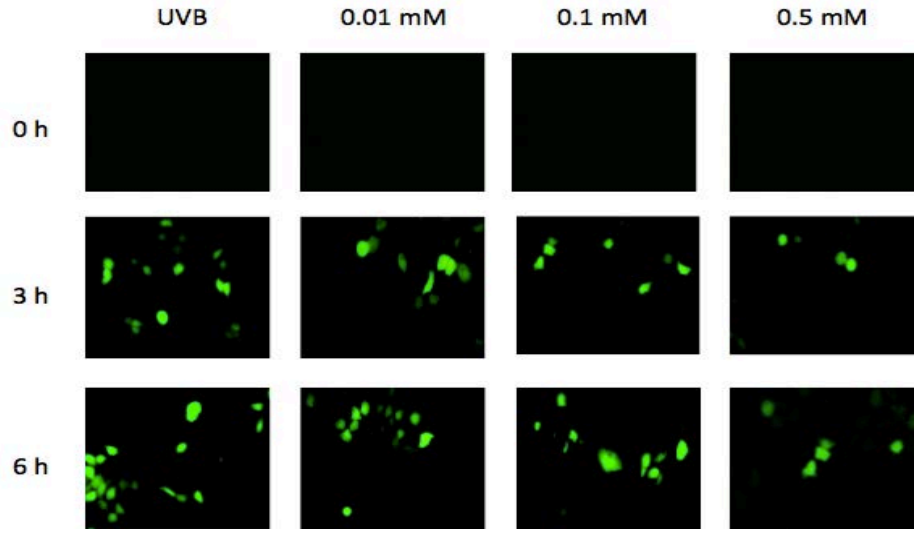

Figure 4.14 Effect of various concentrations of silymarin on ROS production. Cells were treated with 0.01, 0.1, and 0.5 mM of silymarin for 1 h prior to 90 J/m^2 UVB irradiation. A) ROS level was determined by $DCFH_2$-DA probe using fluorescence microplate reader. Data point represent the mean ± S.D. (*n = 4*) *, P < 0.05 versus non-treated cells at the same time point. B) Cellular ROS signal were visualized under fluorescence microscope using ROS detection probe, $DCFH_2$-DA.

4.4 Comparison of known antioxidant effect on oxidative stress induced by UVB in HaCaT cells.

To investigate the effect of vitamin C, vitamin E, and silymarin on ROS generation-induced by UVB exposure, HaCaT cells were incubated with antioxidants at concentration of 0.5 and 0.1 mM for 1 h prior to expose with 90 J/m^2 of UVB. Intracellular ROS was measured by $DCFH_2$-DA as a ROS detection probe and analyzed by fluorescence microplate reader as described.

The results indicated that all antioxidants attenuated the increase of ROS-induced by UVB exposure (Figure 4.15). After UVB (90 J/m^2), the accumulated intracellular ROS was markedly reduced in cells treated with 0.5 mM of antioxidants at all experiment times as compared to non-treated cells exposed to 90 J/m^2 as shown in figure 4.15A. Surprisingly, all antioxidants clearly decrease ROS production to the basal ROS generation as compare to control (0 J/m^2).

The concentration of 0.1 mM antioxidants, silymarin shown the significantly decreased in dose-dependent manner at all experiment times, while vitamin E showed the protective effect in response to ROS during 2 to 6 h and vitamin C had significantly reduced ROS production during 3 to 6 h after UVB exposure as compared to non-treated cells at 90 J/m^2 of UVB (Figure 4.15B), but at dose of 0.1 mM, all antioxidants cannot decrease ROS production to the basal ROS generation as compared to ROS production generated in the control (0 J/m^2).

These results suggested that antioxidants at the concentration of 0.5 and 0.1 mM clearly decreased intracellular ROS-generated by 90 J/m^2 of UVB, but only 0.5 mM of antioxidants decrease the ROS production to the basal ROS. Thus, 0.5 mM was used for find the appropriate kinetic in further experiment.

A.

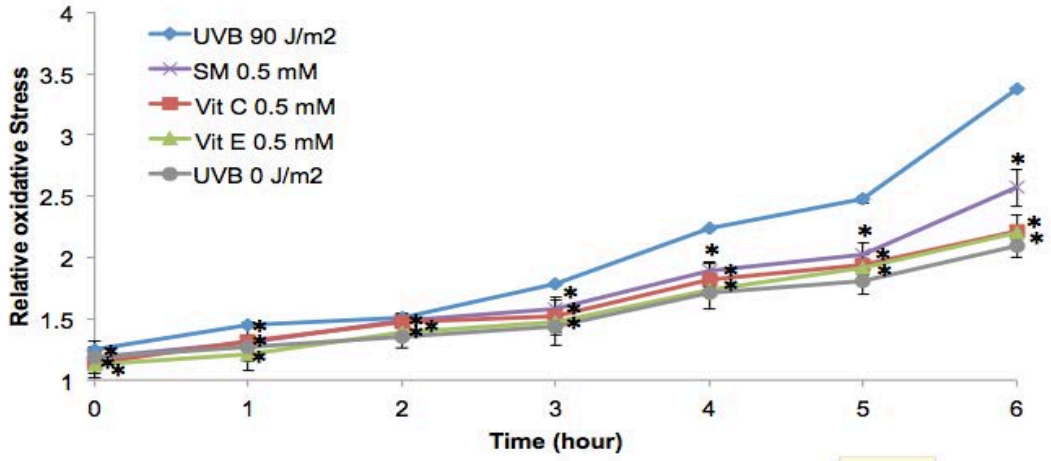

B.

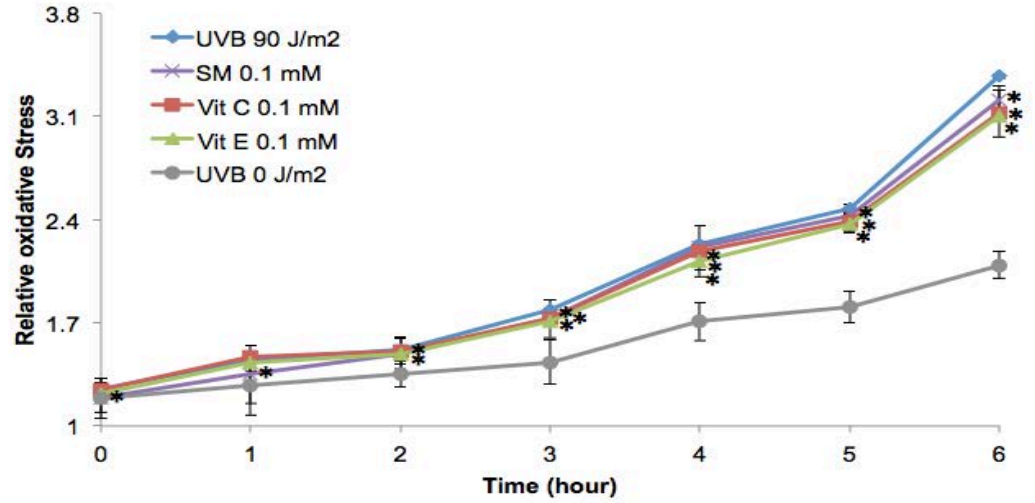

Figure 4.15 Effect of known antioxidants on ROS generated by UVB. A) Cells were treated with 0.5 mM of vitamin C, vitamin E, and silymarin for 1 h before exposed with 90 J/m^2 UVB. B) Cells were treated with 0.1 mM of vitamin C, vitamin E, and silymarin for 1 h before exposed with 90 J/m^2 UVB. Intracellular ROS level was determined by $DCFH_2$-DA probe using fluorescence microplate reader. Data point represent the mean ± S.D. (*n* = *4*) *, P < 0.05 versus non-treated cells at the same time point.

4.5 The kinetics of vitamin C, vitamin E, and silymarin on ROS production in HaCaT cells.

To study the kinetics of vitamin C, vitamin E, and silymarin, cells were incubated with antioxidants at concentration of 0.5 mM for 1 h before exposed to 90 J/m^2 of UVB. The data was plotted representing the intracellular ROS generation in 2 distinguished periods, which were 0-2 h, and 2-6 h. Figure 4.16 demonstrated the graph plotting of ROS signals in the HaCaT in response to UVB versus time.

At the early stage (0-2 h), the results revealed that all antioxidants including control were verified to linear trend line with the R^2 more than 0.97. The highest rate constant value (k) in cells exposed to 90 J/m^2 was approximately 0.1494 with R^2 equal to 0.99427, k value in silymarin treated cells was 0.1438 and R^2 was 0.99653. The k value in vitamin C treated cells was 0.1223 and R^2 was 0.99734. The k value in vitamin E treated cells was 0.0871 and R^2 was 0.99398 and the k value in control (0 J/m^2) was 0.0718 and R^2 was 0.98846, respectively as shown in figure 4.16A. In addition, the k value of vitamin E treated cells exposed to 90 J/m^2 was quite nearly to k value of 0 J/m^2, so the results suggested that cells pretreated with vitamin E exposed to 90 J/m^2 of UVB suppress rate of ROS production to the level of basal ROS generation. Surprisingly, cells pretreated with antioxidants were continuously suppress rate of ROS production up to 6 h as compare to cell exposed to 90 J/m^2 of UVB as shown in figure 4.16B.

These results indicated that all antioxidants down-regulated the intracellular ROS-induced by UVB (90 J/m^2) in human keratinocytes in time-dependent manner. This suppression can be observed in all experiment times as illustrated by kinetic

equations and vitamin E was the effective antioxidant that suppress rate of ROS production to the basal ROS induced by UVB within 2 h after irradiation.

A.

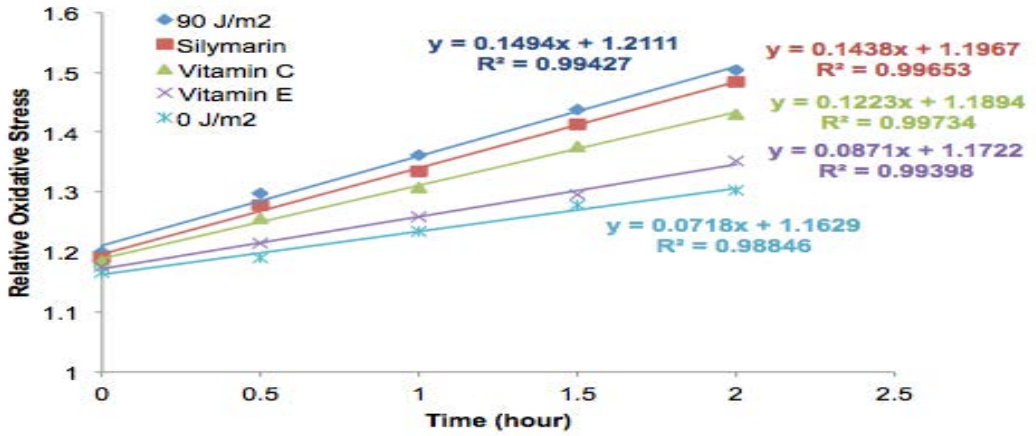

B.

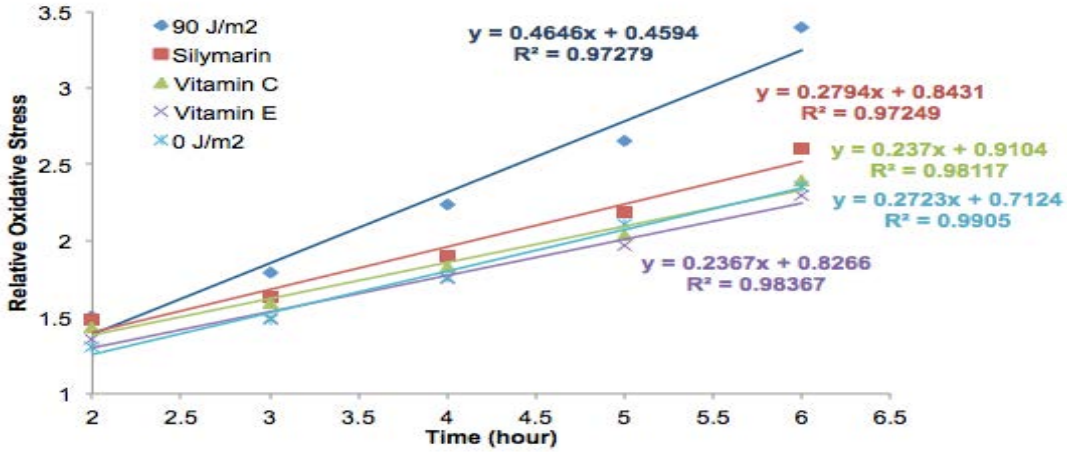

Figure 4.16 Kinetics of well-known antioxidants on ROS signal generated by UVB. A) Kinetics of antioxidants in response to 90 J/m^2 UVB during 0-2 h after UVB irradiation. B) Kinetics of antioxidants in response to 90 J/m^2 UVB during 2-6 h after UVB irradiation. Accumulative intracellular ROS content was evaluated by fluorescence microplate reader, *n = 4*.

5. Investigate on the correlation between the kinetic constant value of ROS and cell death effect

To determine the correlation between kinetic constant value of ROS and cytotoxicity induced by UVB in HaCaT cells, firstly cells were seeded at the density of 10,000 cells per wells in 96 well plate and incubated in serum free condition overnight. After that, cells were exposed with the several doses of UVB (0, 40, 60, 90 J/m^2). The ROS profile of all UVB doses was obtained and generated for an appropriate kinetic constant value during 0-2 h after UVB exposure. The kinetic constant value was plotted versus the percentage of cell viability and apoptosis.

Figure 4.17 demonstrated the correlation between kinetic constant value of intracellular ROS and cell viability and apoptosis at 24 h after UVB exposure. All correlations were fitted with linear equation as $y = \beta x+c$ which were then verified by F test. The analysis will accept the equation if the P value less that significant level (<0.05) as shown in table 1.

These results demonstrated that, base on considering beta value (slope) of correlation equation; apoptosis was the principal mode of cell death induced by ROS generated by UVB.

A.

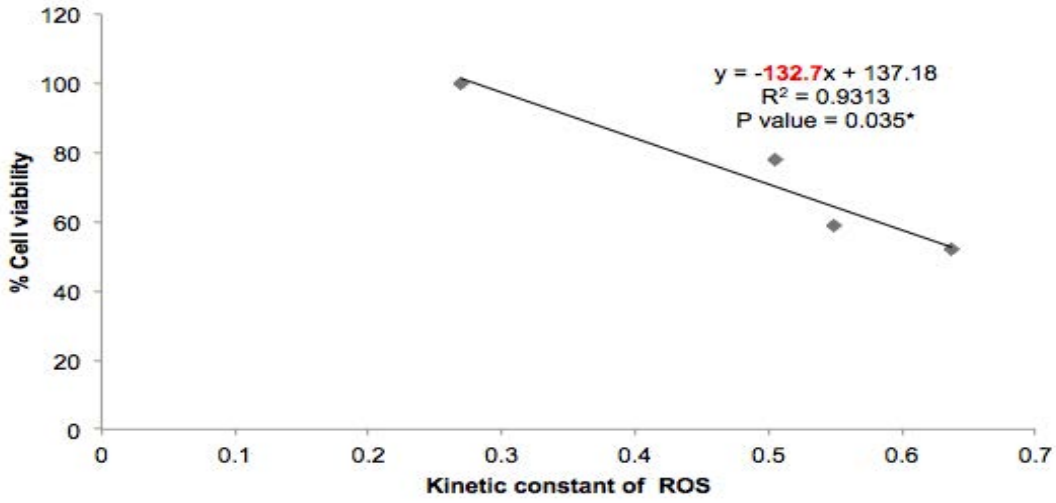

B.

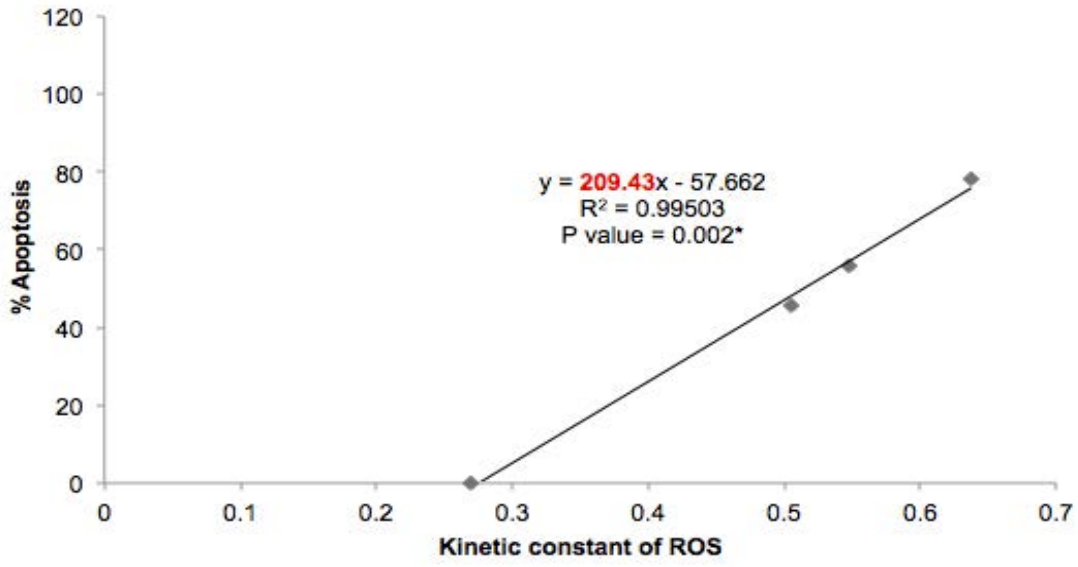

Figure 4.17 The correlation between the rate constant value of ROS and cell death effect induced by UVB. Cells were exposed with several doses of UVB (0, 40, 60, and 90 J/m^2) before examined by MTT and Hoechst 33342 A) The correlation of % cell viability and K value of ROS. B) The correlation of % apoptosis and K value of ROS. Correlation was evaluated by SPSS statistic program (*n = 4*) *, $P < 0.05$.

	Equation	R square	Beta	P value
Cell viability	y = -132.7x+137.18	0.93191	132.7	0.035*
Apoptosis	y = 209.43-57.662	0.99503	209.43	0.002*

Table 1 The linear regression between the rate constant of ROS and cell death effect induced by UVB. This table was demonstrated the equation, R^2, Beta, and P value of cell viability and apoptosis.

CHAPTER V

DISCUSSION AND CONCLUSION

Increasing evidence has supported the significant damaging effects of UVB irradiation on human skin including aging and cancer (Yaar and Gilchrest, 1990; Emerit, 1992; Cleaver and Crowley, 2002; Sander *et al*., 2004). The present study provided information regarding the ROS generating profile in UVB-exposed keratinocytes and reported herein for the first time that superoxide anion and hydroxyl radical are the main specific ROS produced and responsible for oxidative stress in response to UVB.

Oxidative stress caused by the excess amount of intracellular ROS is shown to be an important cause of damage to cellular components. Three main types of ROS were identified and evidence indicated that superoxide anion ($^{\bullet}O_2^-$), hydrogen peroxide (H_2O_2), and hydroxyl radical ($^{\bullet}OH$) were generated continuously in the living cells (Liu *et al*., 2009; Swalwell *et al*., 2011). Superoxide anion after generated could be converted to hydrogen peroxide by the function of superoxide dismutase enzyme. Consistent with this notion, these results revealed that hydrogen peroxide induction in UVB-exposure keratinocytes was found to follow the induction of superoxide anion. However, the increasing level of hydroxyl radical was detectable at the very early time after UVB irritation has indicated the possibility that this free radical may be generated by the direct effect of UVB. Previous study indicated that UVB-mediated damage of pyrimidine base of DNA is tightly associated with cellular oxidative stress (Ichihashi *et al*., 2003; Wiswedel *et al*., 2007; Guo *et al*., 2010). Also,

UVB-induced DNA damage through hydroxyl radical formation was previously demonstrated (Pelle *et al*., 2003).

Although a UVB exposure caused significant ROS up-regulation in keratinocytes up to 24 h (data not shown), this result was found the significant induction of ROS accumulation only at 0-2 h after a UVB exposure compared to that of non-irradiated control. These results probably implied that oxidative stress generated in this study was mediated by the induction of specific ROS in the early time. This study was found that superoxide anion and hydroxyl radical were increased in UVB-treated cells in the higher rate over that of control cells, while a rate of hydrogen peroxide increasing is of minimal difference. Therefore, the results have provided the novel information that oxidative stress caused by UVB is generated at the 2 h-period after exposure by cellular induction of superoxide anion and hydroxyl radical.

Various non-enzymatic dietary antioxidants can protect cells within the body from ROS-induced oxidative damage (Bagchi *et al*., 1999; Al-Gubory *et al*., 2010). Among them, vitamin C is a powerful antioxidant that was shown to reduce an oxidative damage induced by UVB in mouse keratinocytes *in vitro* (Stewart *et al*., 1996). In the present study, vitamin C at the concentration of 0.1, 0.5, and 1 mM could suppress the generation of ROS induced by all doses of UVB irradiation. The effect of vitamin C on ROS generation in response to UVB could be detected as early as 15 min, and the explanation of such prompt effect may be due to the reducing property of vitamin C. Vitamin C was shown to reduce and to maintain function of glutathione in human keratinocytes (Mcardle *et al*., 2002).

Vitamin E is another antioxidant that was shown to protect the human

keratinocytes from UVA-induced lipid peroxidation (Mcardle *et al*., 2002) and also protects the cell membrane from oxidative stress (Traber *et al*., 2007). It has been shown in this study that vitamin E at the non-toxic concentrations (0.1, 0.5, and 1 mM) decreased the intracellular ROS-generated by UVB. Vitamin E seems to be the most effective in protecting ROS generation in comparison to vitamin C and silymarin. These effects may due to vitamin E able to block the lipid peroxidation chain as a soluble lipid-blocking agent (Jin *et al*., 2007).

Previous studies demonstrated that silymarin is the effective antioxidant that protects the oxidative damage in HaCaT cells induced by hydrogen peroxide generated during an UVA exposure (Svobodova *et al*., 2007). In this present study shown that non-toxic doses of silymarin (0.01, 0.1 and 0.5 mM) were able to suppress the ROS induction induced by UVB exposure. Since silymarin has minimal effect on inhibition of superoxide anion generation (Upasani, and Pingale, 2009), a major specific ROS generated by UVB irradiation, this may be the reason why silymarin showed the lowest effective in this study.

Previous research had reported that the intracellular ROS generated by UVB induces apoptosis programmed cell death. The results obtained from the present study had shown reduction in the percentage of cell viability in cells that were exposed with UVB (40, 60, and 90 J/m^2) after 6 hours while the percentage of cell viability of non-irradiated cells stays constant. The correlation identified was used to investigate the ROS factors that play a dominant role in this mechanism. The results demonstrated that apoptosis was the principal mode of cell death induced by ROS production in the early period (0-2 h) of UVB irradiation.

In conclusion, this present study revealed herein the kinetic of ROS generation and identified specific ROS in UVB-exposed human skin keratinocytes. The kinetic plots demonstrated that all antioxidants were able to suppress ROS production in response to UVB in time and dose-dependent manner. These data enhance the understanding on skin biology and benefit the development of strategies in protection of UVB-mediated damages.

References

Agarwal, R., Agarwal, C., Ichikawa, H., Singh, R. P., and Aggarwal, B. B. 2006. Anticancer potential of silymarin: from bench to bed side. Anticancer Res. 26: 4457-4498.

Al-Gubory, K. H., Fowler, P. A., and Garrel, C. 2010. The roles of cellular reactive oxygen species, oxidative stress and antioxidants in pregnancy outcomes. The International Journal of Biochemistry & Cell Biology 42: 1634-1650.

Asghar, Z., and Masood, Z. 2008. Evaluation of antioxidant properties of silymarin and its potential to inhibit peroxyl radicals *in vitro*. Pak J Pharm Sci. 21: 249-254.

Bagchi, M., Balmoori, J., Bagchi, D., Ray, S. D., Kuszynski, C., and Stohs, S. J. 1999. Smokeless tobacco, oxidative stress, apoptosis, and antioxidants in human oral keratinocytes. Free Radical Biology & Medicine 26: 992-1000.

Beaulaton, J., and Lockshin, R. A. 1982. The relation of programmed cell death to development and reproduction: comparative studies and an attempt at classification. Int Rev Cytol. 215-235.

Bender, K., Blattner, C., Knebel, A., Iordanoz, M., Herrlich, P., and Rahmsdorf, H. J. 1997. UV-induced signal transduction. J Photochem Photobiol B. 37: 1-7.

Bielski, B. H., Richter, H. W., and Chan, P. C. 1975. Some properties of the ascorbate free radical. Ann N Y Acad Sci. 258: 231-237.

Buettner, G. R., and Moseley, P. L. 1993. EPR spin trapping of free radicals produced by bleomycin and ascorbate. Free Radic Res Commun. 19: 89-93.

Burton, G. W., Joyce, A., and Ingold, K. U. 1983. Is vitamin E the only lipid-soluble, chain-breaking antioxidant in human blood plasma and erythrocyte membrane. Arch Biochem Biophys. 221: 281-290.

Butterfield, D. A., et al. 1998. Structural and functional changes in proteins induced by free radical-mediated oxidative stress and protective action of the antioxidants *N*-tert-butyl-alpha-phenylnitrone and vitamin E. Ann N Y Acad Sci. 20: 448-462.

Caricchio, R., McPhie, L., and Cohen, P. L. 2003. Ultraviolet B radiation-induced cell death: critical role of ultraviolet dose in inflammation and lupus autoantigen redistribution. J Immunol. 171: 5778-5786.

Chen, Y., Mcmillan-ward, E., Kong, J., Israels, S. J., and Gibson, S. B. 2007. Mitochondrial electron-transport-chain inhibitors of complexes I and II induce autophagic cell death mediated by reactive oxygen species. J Cell Sci. 120: 4155-4166.

Cleaver, J. E., and Crowley, E. 2002. UV damage, DNA repair and skin carcinogenesis. Front Biosci. 7: 1024-1043.

Costin, G. E., and Hearing, V. J. 2007. Human skin pigmentation: melanocytes modulate skin color in response to stress. The Journal of the Federation of American Societies for Experimental Biology 21: 976-994.

Cunningham, M. L., Krinsky, N. I., Giovazzi, S. M., and Peak, M. J. 1985. Superoxide anion is generated from cellular metabolites by solar radiation and its components. J Free Radic Biol Med. 1: 381-385.

Devasagayam, T. P. A., Tilak, J. C., Bollor, K. K., Sane, K. S., Ghaskadbi, S. S., and Lele, R. D. 2004. Free radicals and antioxidants in human health: current status and future prospects. Journal of The Association of Physicians of India 52: 794-804.

Dixit, N., Baboota, S., Kohli, K., Ahmed, S., and Ali, J. 2007. Silymarin: A review of pharmacological aspects and bioavailability enhancement approach. Indian J Pharmacol. 39: 172-179.

Emerit, I. 1992. Free radicals and aging of the skin. EXS. 62: 328-341.

Evans, H. M., and Bishop, K. S. 1922. On the existence of hitherto unrecognized dietary factor essential for reproduction. Science 56: 650-651.

Fehér, J., et al. 1987. Effect of silibinin on the activity and expression of superoxide dismutase in lymphocytes from patients with chronic alcoholic liver disease. Free Radic Res Commun. 3: 373-377.

Fisher, G. J., et al. 1996. Molecular basis of sun-induced premature skin aging and retinoid antagonism. Nature 379: 335-339.

Flora, K., Hahn, M., Rosen, H., and Benner, K. 1998. Milk thistle (Silybum marianum) for the therapy of liver disease. Am J Gastroenterol. 93: 139-43.

Foyer, C. H., Descourvieres, P., and Kunert, K. J. 1994. Protection against oxygen radicals: an important defense mechanism studied in transgenic plants. Plant Cell Environ. 17: 507-523.

Gallucci, S., Lolkema, M., and Matzinger, P. 1999. Natural adjuvants: endogenous activators of dendritic cells. Nat Med. 5(11): 1249-1255.

Garland, C. F., Garland, F. C., and Gorham, E. D. 1993. Rising trends in melanoma: a hypothesis concerning sunscreen effectiveness. Ann Epidermal. 3: 103-110.

Ghosh, A., Ghosh, T., and Jain, S. 2010. Silymarin a review on the pharmacodynamics and bioavailability enhancement approaches. J Pharm sci technol. 2010: 348-355.

Guo, W., An, Y., Jiang, L., Geng, C., and Zhong, L. 2010. The protective effects of hydroxytyrosol against UVB-induced DNA damage in HaCaT cells. Phytotherapy research 24: 352-359.

Gutteridge, J. M. 1982. The role of superoxide and hydroxyl radicals in phospholipid peroxidation catalysed by iron salts. FEBS Lett. 150: 454-458.

Haake, A. R., and Polakowska, R. 1993. Cell death by apoptosis in epidermal biology. J Invest Dermatol. 109: 163-169.

Halliwell, B., and Gutteridge, M. C. 1984. Oxygen toxicity, oxygen radicals, transition metals and disease. Biochem J. 219: 1-14.

Hattori, Y., et al. 1996. Toyokuni, 8-hydroxy-20 -deoxyguanosine is increased in epidermal cells of hairless mice after chronic ultraviolet B exposure. J Invest

Dermatol. 107: 733-737.

Heck, D. E., Vetrano, A. M., Mariano, T. M., and Laskin, J. D. 2003. UVB light stimulates production of reactive oxygen species. The Journal of Biological Chemistry 278(25): 22432-22436.

Ichihashi, M., et al. 2003. UV-induced skin damage. Toxicology 189(1-2): 21-39.

Jadhav, G. B., Upasani, C. D., and Pingale, A. P. 2009. Antioxidant potential of red wine and silymarin: *in-vitro* evaluation. J Pharm Res. 2: 636-639.

Jin, G. H., Liu, Y., Jin, S. Z., Liu, X. D., and Liu, S. Z. 2007. UVB induced oxidative stress in human keratinocytes and protective effect of antioxidant agents. Radiation and Environmental Biophysics 46: 61-68.

Katiyar, S. K., Mantena, S. K., and Meeran, S. M. 2011. Silymarin protects epidermal keratinocytes from ultraviolet radiation-induced apoptosis and DNA damage by nucleotide excision repair mechanism. Plus One 6: 1-11.

Kerr, J. F. R. 1971. Shrinkage necrosis: a distinct mode of cellular death. J Pathol. 105: 13-20.

Kerr, J. F. R., Wyllie, A., and Currie, A. 1972. Apoptosis: a basic biological phenomenon with wide-ranging implications in tissue kinetics. Br J Cancer. 52: 1751-1755.

Kirkinezos, I. G., and Moraes, C. T. 2001. Reactive oxygen species and mitochondrial diseases. Cell Dev Bio. 12: 449-457.

Kovacs, D., et al. 2009. Keratinocyte growth factor down-regulates intracellular ROS production induced by UVB. Journal of Dermatological Science 54: 106-113.

Kraemer, K. H. 1997. Sunlight and skin cancer: another link revealed. Proc Nat Acad Sci USA. 94(1): 11-14.

Kulms, D., Poppelmann, B., Yarosh, D., Luger, T. A., Krutmann, J., and Schwarz, T. 1999. Nuclear and cell membrane effects contribute independently to the induction of apoptosis in human cell exposed to UVB radiation. Proceedings of the National Academy of Sciences of United States of America 96: 7974-7979.

Kulms, D., and Schwarz, T. 2000. Molecular mechanisms of UV-induced apoptosis. Photodermatol Photoimmunol Photomed. 16: 195-201.

Láng, I., Deák, G., Müzes, G., Prónai, L., and Fehér, J. 1993. Effect of natural bioflavonoid antioxidant silymarin on super oxide dismutase (SOD) activity and expression *in vitro*. Biotechnol Ther. 4: 263-270.

Lavker, R., and Matoltsy, A. 1970. Formation of horny cells: the fate of cell organelles and differentiation products in ruminal epithelium. J Cell Biol. 44(3): 501-512.

Lehmann, J., Pollet, D., Peker, S., Steinkraus, V., and Hoppe, U. 1998. Kinetics of DNA strand breaks and protection by antioxidants in UVA- or UVB-irradiated HaCat keratinocytes using the single cell gel electrophoresis assay. Mutation Research 407: 97-108.

Lemoyne, M., Van Gossum, A., Ku-rian, R., and Jeejeebhoy, K. N. 1988. Plasma vitamin E and selenium and breath pentane in home parenteral nutrition patients. Am J Clin Nutr. 48: 1310-1315.

Lemoyne, M., Van Gossum, A., Ku-rian, R., Ostro, M., Axler, J., and Jee-jeebhoy, K. N. 1987. Breath pentane analysis as an index of lipid peroxidation: a functional test of vitamin E status. Am J Clin Nutr. 46: 267-272.

Liebler, D. C., Kling, D. S., and Reed, D. J. 1986. Antioxidant protection of phospholipid bilayers by α-tocopherol. Control of α-tocopherol status by ascorbic and glutathione. J Biol Chem. 261: 12114-12119.

Lisby, S., Gniadecki, R., and Wulf, H. C. 2005. UV-induced DNA damage in human keratinocytes: quantitation and correlation with long-term survival. Exp Dermatol. 14(5): 349-355.

Liu, X., Shi, S., Ye, J., Liu, L., Sun, M., and Wang, C. 2009. Effect of polypeptide from *Chlamys farreri* on UVB-induced ROS/NF-kB/COX-2 activation and apoptosis in HaCat cells. Journal of Photochemistry and Photobiology B: Biology 96: 109-116.

Liu, Y., Fiskum, G., and Schubert, D. 2002. Generation of reactive oxygen species by mitochondrial electron transport chain. J Neurochem. 80(5): 780-787.

Maccubin, A. E., et al. 1995. DNA damage in UVB-irradiated keratinocytes. Carcinogenesis 16(7): 1659-1660.

Mammone, T., Gan, D., Collins, D., Lockshin, R. A., Marenus, K., and Maes, D. 2000. Successful separation of apoptosis and necrosis pathways in HaCaT keratinocyte cells induced by UVB irradiation. Cell Biology and Toxicology 16: 293-302.

Marnett, L. J. 2000. Oxyradicals and DNA damage. Cacinogenesis 21: 361-370.

Martelli, A. M., Zweyer, M., Ochs, R. L., Tazzari, P. L., Narducci, P., and Bortul, R. 2001. Nuclear apoptosis changes: an overview. J Cell Biochem. 82(4): 634-646.

Matito, C., Agell, N., Sanchez-Tena, S., Torres, J. L., and Cascante, M. 2011. Protective effects of structurally diverse grape procyanidin against UV-induced cell damage and cell death. Journal of agricultural and food chemistry 59: 4489-4495.

Mcardle, F., Rhodes, L. E., Parslew, R., Jack, C. I. A., Friedmann, P. S., and Jackson, M. J. 2002. UVR-induced oxidative stress in human skin in vivo: effects of oral vitamin C supplementation. Free Radical Biology & Medicine 33: 1355-1362.

Mira, L., Silva, M., and Manso, C. F. 1994. Scavenging of reactive oxygen species by silibinin dihemisuccinate. Biochem Pharmacol. 48: 753-759.

Muriel, P., Garciapina, T., Perez-Alvarez, V., and Mourelle, M. 1992. Silymarin protects against paracetamol-induced lipid peroxidation and liver damage. J Appl Toxicol. 12: 439-442.

Nordberg, J., and Arner, E. S. J. 2001. Reactive oxygen species, antioxidants and the mammalian thioredoxin system. Free Radical Biol Med. 31: 1287-1312.

Padh, H. 1990. Cellular functions of ascorbic acid. Biochem Cell Biol. 68: 1166-1173.

Pelle, E., Huang, X., Mamone, T., Marenus, K., Maes, D., and Frenkel, K. 2003. Ultraviolet-B-induced oxidative DNA base damage in primary normal human epidermal keratinocytes and inhibit by a hydroxyl radical scavenger. J Invest Dermatol. 121(1): 177-183.

Pham-Huy, L. A., He, H., and Pham-Huy, C. 2008. Free Radicals, Antioxidants in Disease and Health, Int J Biomed Sci. 4: 89-96.

Saitoh, Y., et al. 2011. Super-highly hydroxylated fullerene derivative protects human keratinocytes from UV-induced cell injuries together with the decreases in intracellular ROS generation and DNA damages. Journal of Photochemistry and Photobiology B: Biology 102: 69-76.

Salganik, R. I. 2001. The benefits and hazards of antioxidants: controlling apoptosis and other protective mechanisms in cancer patients and the human population. J Am Coll Nutr. 20(5): 464-472.

Saliou, C., et al. 1998. Antioxidants modulate acute solar ultraviolet radiation-induced NF-KAPPA-B activation in a human keratinocyte cell line. Free radical biology and medicine 26: 174-183.

Saller, R., Meier, R., and Brignoli, R. 2001. The use of silymarin in the treatment of liver diseases. Drugs 61: 2035-2063.

Sander, C. S., Chang, H., Hamm, F., Elsner, P., and Thiele, J. J. 2004. Role of oxidative stress and the antioxidant network in cutaneous carcinogenesis. Int J Dermatol. 43: 326-335.

Santa-Maria, C., et al. 2010. Protective against free radicals (UVB irradiation) of a water-soluble enzymatic extract from rice bran. Study using human keratinocyte monolayer and reconstructed human epidermis. Food and Chemical Toxicology 48: 83-88.

Savini, I., D'Angelo, I., Ranalli, M., Melino, G., and Avigliano, L. 1999. Ascorbic acid maintenance in HaCaT cells prevents radical formation and apoptosis by UV-B. Free Radic Biol Med. 26: 1172-1180.

Scharffetter-Kochanek, K., Wlaschek, M., Brenneisen, P., Schauen, M., Blaudschun, R., and Wenk, J. 1997. UV-induced reactive oxygen species in photocarcinogenesis and photoaging. Biol Chem. 378: 1247-1257.

Sebastian, J., et al. 2003. Vitamin C as an antioxidant: evaluation of its role in disease prevention. Journal of the American college of nutrition 22(1): 18-35.

Sinha R. P., and Hader, D. P. 2002. UV-induced DNA damage and repair: a review. Photochem Photobiol Sci. 1: 225-236.

Sonnenbichler, J., Scalera, F., Sonnenbichler, I., and Weyhenmeyer, R. 1999. Stimulatory effects of silibinin and silicristin from the milk thistle Silybum marianum on kidney cells. J Pharmacol Exp Ther. 290: 1375-1383.

Suzuki, Y. J., et al. 1993. Structural and dynamic membrane properties of alpha-tocopherol and alpha-tocotrienol: implication to the molecular mechanism of their antioxidant potency. Biochemistry 32: 10692-10699.

Svobodová, A., Walterová, D., and Psotová, J. 2007. Influence of silymarin and its flavonolignans on H_2O_2-induced oxidative stress in human keratinocytes and mouse fibroblasts. Burns 32: 973-979.

Swalwell, H., Latimer, J., Haywood, R. M., and Birch-Machin, M. A. 2011. Investigating the role of melanin in UVA/UVB- and hydrogen peroxide-induced cellular and mitochondrial ROS production and mitochondrial DNA damage in human melanoma cells. Free Radical Biology & Medicine 52: 626-634.

Tejero, I., Gonzalez-Lafont, A., Lluch, J. M., and Eriksson, L. A. 2007. Theoretical modeling of hydroxyl-radical-induced lipid peroxidation reactions. J Phys Chem B. 111: 5684-5693.

Thannickal, V. J., and Fanburg, B. L. 2000. Reactive oxygen species in cell signaling. Am J Physiol Lung Cell Mol Physiol. 279: 1005-1028.

Traber, M. G., and Atkinson, J. 2007. Vitamin E, antioxidant and nothing more. Free Radical & Medicine 43: 4-15.

Tyrrell, R. M. 1996. Activation of mammalian gene expression by UV component of sunlight from models to reality. Bioessays 18: 139-148.

Valenzuela, A., Aspillaga, M., Vial, S., and Guerra, R. 1989. Selectivity of silymarin on the increase of the glutathione content in different tissues of the rat. Planta Med. 55: 420-422.

Valenzuela, A., Lagos, C., Schmidt, K., and Videla, L. A. 1985. Silymarin protection against hepatic lipid peroxidation induced by acute ethanol intoxication in the rat. Biochem Pharmacol. 34: 2209-2212.

Valko, M., et al. 2007. Free radicals and antioxidants in normal physiological functions and human disease. Int J Biochem Cell Biol. 39: 44-84.

Wang, H., and Kochevar, I. E. 2005. Involvement of UVB-induced reactive oxygen species in TGF-β biosynthesis and activation in keratinocytes. Free Radical Bio Med. 38: 890-897.

Washko, P. W., Wnag, Y., and Levine, M. 1993. Ascorbic acid recycling in human neutrophils. J Biol Chem. 268: 15531-15535.

Yaar, M., and Gilchrest, B. A. 1990. Cellular and molecular mechanisms of cutaneous againg. J Dermatol Surg Oncol. 16: 915-922.

Young, A. R. 1987. The sunburn cell. Photodermatology 4(3): 127-134.

Young, I. S., and Woodside, J. V. 2001. Antioxidants in health and disease. J Clin Pathol. 54: 176-86.

APPENDIX

APPENDIX

TABLES OF EXPERIMENTAL RESULTS

Table 2 The percentage of cell survival after exposed with several doses of UVB was evaluated by MTT assay at the end of each time point (time dependency).

Time (hour)	Cell viability (%)			
	0 J/m^2	40 J/m^2	60 J/m^2	90 J/m^2
0	100.00 ± 0.00	99.25 ± 0.04	99.29 ± 0.01	99.25 ± 0.07
6	100.00 ± 0.00	86.97 ± 4.23*	82.41 ± 5.48*	74.68 ± 4.79*
12	100.00 ± 0.00	82.18 ± 2.17*	65.11 ± 3.75*	57.47 ± 2.67*
24	100.00 ± 0.00	77.89 ± 2.61*	58.72 ± 1.27*	51.89 ± 2.69*

Each value represents the mean ± S.D. of four independent experiments. Symbols refer significant different from the control group (time = 0 h): *, $p < 0.05$ determined by One-way ANOVA.

Table 3 ROS intensity of HaCaT cells after exposed with several doses of UVB using $DCFH_2$-DA probe (time dependency).

Time (hour)	Relative DCF intensity			
	0 J/m^2 (control)	40 J/m^2	60 J/m^2	90 J/m^2
0	0.99 ± 0.03	0.99 ± 0.06	1.01 ± 0.06	1.07 ± 0.03
1	1.30 ± 0.03	1.42 ± 0.07*	1.57 ± 0.05*	1.72 ± 0.05*
2	1.48 ± 0.04	1.95 ± 0.05*	2.13 ± 0.05*	2.31 ± 0.07*
3	1.64 ± 0.03	2.22 ± 0.05*	2.42 ± 0.09*	2.65 ± 0.09*
4	1.86 ± 0.02	2.46 ± 0.05*	2.68 ± 0.08*	2.92 ± 0.09*
5	2.04 ± 0.03	2.65 ± 0.05*	2.85 ± 0.07*	3.05 ± 0.08*
6	2.22 ± 0.03	2.82 ± 0.06*	3.05 ± 0.08*	3.28 ± 0.08*

The DCF signal of each dose at each time point was normalized to non-irradiation cells and reported as relative DCF intensity. Each value represents the mean ± S.D. of four independent experiments. Symbols refer significant different from the control group (0 J/m^2): *, $p < 0.05$ determined by One-way ANOVA.

Table 4 ROS intensity of HaCaT cells after exposed with several doses of UVB by using $DCFH_2$-DA probe (time dependency). Accumulative intracellular ROS content was evaluated using fluorescence microplate reader. Each value represents the mean ± S.D. of four independent experiments. This result was used for finding kinetic equation.

Time (hour)	Relative DCF intensity			
	0 J/m^2 (control)	40 J/m^2	60 J/m^2	90 J/m^2
0	1.00 ± 0.00	1.01 ± 0.10	1.02 ± 0.10	1.04 ± 0.02
0.5	1.20 ± 0.10	1.36 ± 0.10	1.44 ± 0.11	1.52 ± 0.02
1	1.35 ± 0.11	1.53 ± 0.01	1.70 ± 0.10	1.82 ± 0.05
1.5	1.45 ± 0.10	1.80 ± 0.01	1.95 ± 0.10	2.11 ± 0.05
2	1.55 ± 0.10	2.06 ± 0.05	2.14 ± 0.05	2.35 ± 0.01
3	1.64 ± 0.40	2.10 ± 0.05	2.42 ± 0.09	2.65 ± 0.01
4	1.86 ± 0.23	2.22 ± 0.05	2.68 ± 0.07	2.92 ± 0.08
5	2.04 ± 0.12	2.46 ± 0.05	2.85 ± 0.07	3.05 ± 0.09
6	2.22 ± 0.45	2.82 ± 0.06	3.05 ± 0.08	3.28 ± 0.08

Table 5 Specific hydroxyl radical intensity of HaCaT cells after exposed with various doses of UVB and determined by using HPF as a specific probe.

Time (hour)	Relative HPF intensity			
	0 J/m^2 (control)	40 J/m^2	60 J/m^2	90 J/m^2
0	1.01 ± 0.01	1.06 ± 0.04*	1.06 ± 0.04*	1.07 ± 0.04*
1	1.02 ± 0.02	1.12 ± 0.02*	1.21 ± 0.03*	1.36 ± 0.02*
2	1.06 ± 0.02	1.20 ± 0.04*	1.27 ± 0.03*	1.44 ± 0.03*
3	1.24 ± 0.05	1.29 ± 0.04*	1.36 ± 0.03*	1.45 ± 0.01*
4	1.33 ± 0.04	1.43 ± 0.05*	1.47 ± 0.04*	1.49 ± 0.02*
5	1.34 ± 0.04	1.44 ± 0.06*	1.50 ± 0.05*	1.56 ± 0.04*
6	1.37 ± 0.03	1.45 ± 0.05*	1.51 ± 0.05*	1.62 ± 0.05*

The HPF signal of each dose at each time point was normalized to non-irradiation cells and reported as relative HPF intensity. Each value represents the mean ± S.D. of four independent experiments. Symbols refer significant different from the control group (0 J/m^2): *, $p < 0.05$ determined by One-way ANOVA.

Table 6 Specific hydrogen peroxide intensity of HaCaT cells after exposed with various doses of UVB and determined by using Amplex Red as a specific probe.

Time (hour)	Relative Amplex Red intensity			
	0 J/m^2 (control)	40 J/m^2	60 J/m^2	90 J/m^2
0	1.00 ± 0.02	1.33 ± 0.06*	1.42 ± 0.04*	1.49 ± 0.03*
1	1.69 ± 0.05	1.87 ± 0.06*	1.91 ± 0.09*	1.96 ± 0.05*
2	2.26 ± 0.10	2.47 ± 0.07*	2.72 ± 0.12*	2.77 ± 0.11*
3	2.91 ± 0.12	3.31 ± 0.13*	3.68 ± 0.17*	4.00 ± 0.26*
4	3.62 ± 0.24	4.24 ± 0.26*	4.57 ± 0.24*	5.23 ± 0.41*
5	4.38 ± 0.31	4.89 ± 0.38*	5.50 ± 0.65*	6.17 ± 0.47*
6	5.29 ± 0.36	5.90 ± 0.45*	6.56 ± 0.58*	7.31 ± 0.62*

The Amplex Red signal of each dose at each time point was normalized to non-irradiation cells and reported as relative Amplex Red intensity. Each value represents the mean ± S.D. of four independent experiments. Symbols refer significant different from the control group (0 J/m^2): *, $p < 0.05$ determined by One-way ANOVA.

Table 7 Specific superoxide intensity of HaCaT cells after exposed with various doses of UVB and determined by using DHE as a specific probe.

Time (hour)	Relative DHE intensity			
	0 J/m^2 (control)	40 J/m^2	60 J/m^2	90 J/m^2
0	1.00 ± 0.01	1.07 ± 0.04*	1.11 ± 0.02*	1.17 ± 0.04*
1	1.22 ± 0.14	1.58 ± 0.06*	1.59 ± 0.06*	2.18 ± 0.16*
2	2.45 ± 0.13	3.77 ± 0.20*	3.97 ± 0.18*	4.44 ± 0.10*
3	3.58 ± 0.20	4.30 ± 0.16*	4.55 ± 0.30*	5.26 ± 0.19*
4	4.06 ± 0.30	4.65 ± 0.23*	4.84 ± 0.27*	5.38 ± 0.16*
5	4.18 ± 0.30	4.83 ± 0.26*	5.11 ± 0.21*	5.61 ± 0.17*
6	4.20 ± 0.27	4.88 ± 0.26*	5.17 ± 0.17*	5.79 ± 0.20*

The DHE signal of each dose at each time point was normalized to non-irradiation cells and reported as relative DHE intensity. Each value represents the mean ± S.D. of four independent experiments. Symbols refer significant different from the control group (0 J/m^2): *, $p < 0.05$ determined by One-way ANOVA.

Table 8 Specific hydroxyl radical intensity of HaCaT cells after exposed to 90 J/m^2 UVB and determined by using HPF as a specific probe. Accumulative specific ROS content was evaluated using fluorescence microplate reader. Each value represents the mean ± S.D. of four independent experiments.

Time (hour)	Relative fluorescence intensity
	HPF + 90 J/m^2 UVB
0	1.17 ± 0.01
0.5	1.28 ± 0.01
1	1.37 ± 0.05
1.5	1.40 ±0.05
2	1.45 ± 0.10
3	1.47 ± 0.12
4	1.51 ± 0.01
5	1.56 ± 0.04
6	1.62 ± 0.04

Table 9 Specific hydrogen peroxide intensity of HaCaT cells after exposed to 90 J/m^2 UVB and determined by using Amplex Red as a specific probe. Accumulative specific ROS content was evaluated using fluorescence microplate reader. Each value represents the mean ± S.D. of four independent experiments.

Time (hour)	Relative fluorescence intensity
	Amplex Red + 90 J/m^2 UVB
0	1.52 ± 0.19
0.5	1.70 ± 0.10
1	1.98 ± 0.02
1.5	2.40 ± 0.02
2	2.79 ± 0.04
3	4.18 ± 0.04
4	5.23 ± 0.01
5	6.17 ± 0.03
6	7.31 ± 0.01

Table 10 Specific superoxide anion intensity of HaCaT cells after exposed to 90 J/m^2 UVB and determined by using DHE as a specific probe. Accumulative specific ROS content was evaluated using fluorescence microplate reader. Each value represents the mean ± S.D. of four independent experiments.

Time (hour)	Relative fluorescence intensity
	DHE + 90 J/m^2 UVB
0	1.18 ± 0.04
0.5	1.70 ± 0.04
1	2.24 ± 0.01
1.5	3.10 ± 0.01
2	4.54 ± 0.02
3	5.26 ± 0.01
4	5.38 ± 0.02
5	5.61 ± 0.01
6	5.76 ± 0.01

Table 11 The percentage of HaCaT cell viability was determined by MTT assay after treatment with various concentrations of vitamin C for 24 h (dose dependency).

Vitamin C (mM)	Cell viability (%)
control	100 ± 1.54
0.1	99.75 ± 1.11
0.5	99.48 ± 1.11
1	98.01 ± 3.12
2.5	66.78 ± 4.21*
5	52.00 ± 2.25*
10	40.56 ± 1.08*

Each value represents the mean ± S.D. of four independent experiments. Symbols refer significant different from the control group: *, $p < 0.05$ determined by One-way ANOVA.

Table 12 ROS intensity of HaCaT cells after pretreatment with 0.1 mM of vitamin C prior to exposed with several doses of UVB and determined by using $DCFH_2$-DA probe.

Time (hour)	Relative DCF intensity			
	0.1 mM vit C + 0 J/m^2 (control)	0.1 mM vit C + 40 J/m^2	0.1 mM vit C + 60 J/m^2	0.1 mM vit C + 90 J/m^2
0	1.00 ± 0.07	1.03 ± 0.03	1.04 ± 0.02	1.24 ± 0.08*
1	1.04 ± 0.05	1.09 ± 0.08*	1.33 ± 0.12*	1.46 ± 0.02*
2	1.05 ± 0.01	1.12 ± 0.11*	1.41 ± 0.10*	1.51 ± 0.09*
3	1.46 ± 0.02	1.51 ± 0.05*	1.63 ± 0.03*	1.72 ± 0.13*
4	1.82 ± 0.01	1.94 ± 0.10*	2.05 ± 0.16*	2.18 ± 0.17*
5	2.13 ± 0.02	2.18 ± 0.04*	2.19 ± 0.09*	2.38 ± 0.06*
6	2.41 ± 0.05	2.50 ± 0.13*	2.78 ± 0.11*	3.11 ± 0.15*

The DCF signal of each dose at each time point was normalized to non-irradiation cells and reported as relative DCF intensity. Each value represents the mean ± S.D. of four independent experiments. Symbols refer significant different from the control group: *, $p < 0.05$ determined by One-way ANOVA.

Table 13 ROS intensity of HaCaT cells after pretreatment with 0.5 mM of vitamin C prior to exposed with several doses of UVB and determined by using $DCFH_2$-DA probe.

Time (hour)	Relative DCF intensity			
	0.5 mM vit C + 0 J/m^2 (control)	0.5 mM vit C + 40 J/m^2	0.5 mM vit C + 60 J/m^2	0.5 mM vit C + 90 J/m^2
0	1.00 ± 0.01	1.03 ± 0.01	1.07 ± 0.02*	1.13 ± 0.11*
1	1.00 ± 0.05	1.04 ± 0.02*	1.27 ± 0.06*	1.31 ± 0.05*
2	1.06 ± 0.01	1.14 ± 0.07*	1.30 ± 0.09*	1.47 ± 0.05*
3	1.21 ± 0.01	1.30 ± 0.02*	1.48 ± 0.17*	1.52 ± 0.15*
4	1.32 ± 0.03	1.57 ± 0.06*	1.73 ± 0.13*	1.82 ± 0.13*
5	1.57 ± 0.07	1.63 ± 0.08*	1.83 ± 0.13*	1.93 ± 0.08*
6	1.80 ± 0.03	1.94 ± 0.09*	2.13 ± 0.10*	2.21 ± 0.13*

The DCF signal of each dose at each time point was normalized to non-irradiation cells and reported as relative DCF intensity. Each value represents the mean ± S.D. of four independent experiments. Symbols refer significant different from the control group: *, $p < 0.05$ determined by One-way ANOVA.

Table 14 ROS intensity of HaCaT cells after pretreatment with 1 mM of vitamin C prior to exposed with several doses of UVB and determined by using $DCFH_2$-DA probe.

Time (hour)	Relative DCF intensity			
	1 mM vit C + 0 J/m^2 (control)	1 mM vit C + 40 J/m^2	1 mM vit C + 60 J/m^2	1 mM vit C + 90 J/m^2
0	1.00 ± 0.01	1.00 ± 0.04	1.08 ± 0.01*	1.08 ± 0.06*
1	1.01 ± 0.07	1.04 ± 0.04*	1.20 ± 0.05*	1.26 ± 0.07*
2	1.01 ± 0.06	1.04 ± 0.04*	1.25 ± 0.11*	1.36 ± 0.05*
3	1.10 ± 0.06	1.25 ± 0.04*	1.39 ± 0.10*	1.47 ± 0.16*
4	1.24 ± 0.05	1.48 ± 0.02*	1.69 ± 0.09*	1.79 ± 0.22*
5	1.52 ± 0.07	1.62 ± 0.07*	1.77 ± 0.03*	1.87 ± 0.06*
6	1.81 ± 0.09	1.85 ± 0.01*	2.03 ± 0.04*	2.16 ± 0.03*

The DCF signal of each dose at each time point was normalized to non-irradiation cells and reported as relative DCF intensity. Each value represents the mean ± S.D. of four independent experiments. Symbols refer significant different from the control group: *, $p < 0.05$ determined by One-way ANOVA.

Table 15 ROS intensity of HaCaT cells after pretreatment with various concentrations of vitamin C prior to exposed with 90 J/m^2 UVB and determined by using $DCFH_2$-DA probe.

Time (hour)	Relative DCF intensity			
	control (90J/m^2)	0.1 mM vit C + 90J/m^2	0.5 mM vit C + 90J/m^2	1 mM vit C + 90J/m^2
0	1.25 ± 0.01	1.24 ± 0.08	1.13 ± 0.11*	1.22 ± 0.06*
1	1.45 ± 0.01	1.46 ± 0.02	1.31 ± 0.05*	1.42 ± 0.07*
2	1.51 ± 0.01	1.51 ± 0.09	1.47 ± 0.05*	1.48 ± 0.05*
3	1.78 ± 0.01	1.72 ± 0.13*	1.52 ± 0.15*	1.52 ± 0.16*
4	2.23 ± 0.01	2.18 ± 0.17*	1.82 ± 0.13*	1.82 ± 0.22*
5	2.47 ± 0.03	2.38 ± 0.06*	1.93 ± 0.08*	1.93 ± 0.06*
6	3.37 ± 0.01	3.11 ± 0.15*	2.21 ± 0.13*	2.21 ± 0.03*

The DCF signal of each dose at each time point was normalized to non-treated cells and reported as relative DCF intensity. Each value represents the mean ± S.D. of four independent experiments. Symbols refer significant different from the control group: *, $p < 0.05$ determined by One-way ANOVA.

Table 16 The percentage of HaCaT cell viability was determined by MTT assay after treatment with various concentrations of vitamin E for 24 h (dose dependency).

Vitamin E (mM)	Cell viability (%)
control	100 ± 2.86
0.1	103.05 ± 3.98
0.5	101.49 ± 1.06
1	99.06 ± 3.06
2.5	80.91 ± 2.15*
5	75.43 ± 4.02*
10	70.90 ± 5.94*

Each value represents the mean ± S.D. of four independent experiments. Symbols refer significant different from the control group: *, $p < 0.05$ determined by One-way ANOVA.

Table 17 ROS intensity of HaCaT cells after pretreatment with 0.1 mM of vitamin E prior to exposed with several doses of UVB and determined by using $DCFH_2$-DA probe.

Time (hour)	Relative DCF intensity			
	0.1 mM vit E + 0 J/m^2 (control)	0.1 mM vit E + 40 J/m^2	0.1 mM vit E + 60 J/m^2	0.1 mM vit E + 90 J/m^2
0	1.00 ± 0.01	1.00 ± 0.03	1.06 ± 0.01*	1.22 ± 0.01*
1	1.01 ± 0.07	1.07 ± 0.08*	1.31 ± 0.06*	1.42 ± 0.05*
2	1.05 ± 0.08	1.10 ± 0.06*	1.37 ± 0.12*	1.48 ± 0.01*
3	1.43 ± 0.02	1.52 ± 0.03*	1.61 ± 0.08*	1.71 ± 0.02*
4	1.77 ± 0.01	1.92 ± 0.05*	2.03 ± 0.05*	2.12 ± 0.06*
5	2.09 ± 0.06	2.15 ± 0.07*	2.18 ± 0.04*	2.36 ± 0.05*
6	2.40 ± 0.03	2.48 ± 0.03*	2.76 ± 0.02*	3.10 ± 0.01*

The DCF signal of each dose at each time point was normalized to non-irradiation cells and reported as relative DCF intensity. Each value represents the mean ± S.D. of four independent experiments. Symbols refer significant different from the control group: *, $p < 0.05$ determined by One-way ANOVA.

Table 18 ROS intensity of HaCaT cells after pretreatment with 0.5 mM of vitamin E prior to exposed with several doses of UVB and determined by using $DCFH_2$-DA probe.

Time (hour)	Relative DCF intensity			
	0.5 mM vit E + 0 J/m^2 (control)	0.5 mM vit E + 40 J/m^2	0.5 mM vit E + 60 J/m^2	0.5 mM vit E + 90 J/m^2
0	1.00 ± 0.01	0.99 ± 0.03	1.03 ± 0.01	1.12 ± 0.01*
1	1.04 ± 0.13	1.04 ± 0.07	1.14 ± 0.02*	1.20 ± 0.05*
2	1.06 ± 0.13	1.07 ± 0.06	1.24 ± 0.04*	1.39 ± 0.05*
3	1.33 ± 0.09	1.37 ± 0.07*	1.42 ± 0.01*	1.47 ± 0.08*
4	1.35 ± 0.09	1.52 ± 0.24*	1.68 ± 0.03*	1.74 ± 0.01*
5	1.58 ± 0.09	1.68 ± 0.07*	1.80 ± 0.01*	1.91 ± 0.01*
6	1.80 ± 0.02	1.92 ± 0.01*	2.11 ± 0.05*	2.19 ± 0.04*

The DCF signal of each dose at each time point was normalized to non-irradiation cells and reported as relative DCF intensity. Each value represents the mean ± S.D. of four independent experiments. Symbols refer significant different from the control group: *, $p < 0.05$ determined by One-way ANOVA.

Table 19 ROS intensity of HaCaT cells after pretreatment with 1 mM of vitamin E prior to exposed with several doses of UVB and determined by using $DCFH_2$-DA probe.

Time (hour)	Relative DCF intensity			
	1 mM vit E + 0 J/m^2 (control)	1 mM vit E + 40 J/m^2	1 mM vit E + 60 J/m^2	1 mM vit E + 90 J/m^2
0	1.00 ± 0.00	0.99 ± 0.03	1.03 ± 0.01	1.11 ± 0.01*
1	1.02 ± 0.12	1.03 ± 0.03	1.10 ± 0.11*	1.11 ± 0.10*
2	1.05 ± 0.05	1.05 ± 0.10	1.18 ± 0.11*	1.32 ± 0.05*
3	1.24 ± 0.02	1.33 ± 0.06*	1.32 ± 0.06*	1.45 ± 0.05*
4	1.32 ± 0.09	1.45 ± 0.10*	1.54 ± 0.06*	1.67 ± 0.02*
5	1.43 ± 0.04	1.50 ± 0.06*	1.76 ± 0.05*	1.85 ± 0.07*
6	1.76 ± 0.05	1.83 ± 0.03*	2.01± 0.13*	2.12 ± 0.08*

The DCF signal of each dose at each time point was normalized to non-irradiation cells and reported as relative DCF intensity. Each value represents the mean ± S.D. of four independent experiments. Symbols refer significant different from the control group: *, $p < 0.05$ determined by One-way ANOVA.

Table 20 ROS intensity of HaCaT cells after pretreatment with various concentrations of vitamin E prior to exposed with 90 J/m^2 UVB and determined by using $DCFH_2$-DA probe.

Time (hour)	Relative DCF intensity			
	control (90J/m^2)	0.1 mM vit E + 90J/m^2	0.5 mM vit E + 90J/m^2	1 mM vit E + 90J/m^2
0	1.25 ± 0.01	1.22 ± 0.01	1.12 ± 0.01*	1.11 ± 0.01*
1	1.45 ± 0.01	1.42 ± 0.05	1.20 ± 0.05*	1.11 ± 0.10*
2	1.51 ± 0.01	1.48 ± 0.01*	1.39 ± 0.05*	1.32 ± 0.05*
3	1.78 ± 0.01	1.71 ± 0.02*	1.47 ± 0.08*	1.45 ± 0.05*
4	2.23 ± 0.01	2.12 ± 0.06*	1.74 ± 0.01*	1.67 ± 0.02*
5	2.47 ± 0.03	2.36 ± 0.05*	1.91 ± 0.01*	1.85 ± 0.07*
6	3.37 ± 0.01	3.10 ± 0.01*	2.19 ± 0.04*	2.12 ± 0.08*

The DCF signal of each dose at each time point was normalized to non-treated cells and reported as relative DCF intensity. Each value represents the mean ± S.D. of four independent experiments. Symbols refer significant different from the control group: *, $p < 0.05$ determined by One-way ANOVA.

Table 21 The percentage of HaCaT cell viability was determined by MTT assay after treatment with various concentrations of silymarin for 24 h (dose dependency).

Silymarin (mM)	Cell viability (%)
control	100 ± 7.02
0.01	103.48 ± 5.05
0.1	102.34 ± 3.04
0.5	99.12 ± 3.02
1	74.29 ± 1.01*
2.5	52.43 ± 4.01*
5	24.53 ± 5.08*

Each value represents the mean ± S.D. of four independent experiments. Symbols refer significant different from the control group: *, $p < 0.05$ determined by One-way ANOVA.

Table 22 ROS intensity of HaCaT cells after pretreatment with 0.01 mM of silymarin prior to exposed with several doses of UVB and determined by using $DCFH_2$-DA probe.

Time (hour)	Relative DCF intensity			
	0.01 mM SM + 0 J/m^2 (control)	0.01 mM SM + 40 J/m^2	0.01 mM SM + 60 J/m^2	0.01 mM SM + 90 J/m^2
0	1.00 ± 0.03	1.03 ± 0.09	1.08 ± 0.11*	1.23 ± 0.11*
1	1.03 ± 0.10	1.08 ± 0.10*	1.33 ± 0.30*	1.43 ± 0.12*
2	1.11 ± 0.05	1.19 ± 0.06*	1.41 ± 0.06*	1.51 ± 0.04*
3	1.45 ± 0.07	1.56 ± 0.05*	1.65 ± 0.11*	1.76 ± 0.01*
4	1.79 ± 0.06	1.97 ± 0.03*	2.13 ± 0.05*	2.21 ± 0.02*
5	2.06 ± 0.10	2.19 ± 0.08*	2.21 ± 0.10*	2.45 ± 0.18*
6	2.41 ±0.02	2.59 ± 0.13*	2.83 ± 0.08*	3.27 ± 0.08*

The DCF signal of each dose at each time point was normalized to non-irradiation cells and reported as relative DCF intensity. Each value represents the mean ± S.D. of four independent experiments. Symbols refer significant different from the control group: *, $p < 0.05$ determined by One-way ANOVA.

Table 23 ROS intensity of HaCaT cells after pretreatment with 0.1 mM of silymarin prior to exposed with several doses of UVB and determined by using $DCFH_2$-DA probe.

Time (hour)	Relative DCF intensity			
	0.1 mM SM + 0 J/m^2 (control)	0.1 mM SM + 40 J/m^2	0.1 mM SM + 60 J/m^2	0.1 mM SM + 90 J/m^2
0	1.00 ± 0.03	1.03 ± 0.07	1.08 ± 0.11*	1.19 ± 0.09*
1	1.04 ± 0.05	1.07 ± 0.05*	1.33 ± 0.06*	1.35 ± 0.19*
2	1.08 ± 0.08	1.12 ± 0.04*	1.41 ± 0.05*	1.48 ± 0.10*
3	1.43 ± 0.08	1.53 ± 0.12*	1.63 ± 0.14*	1.73 ± 0.03*
4	1.77 ± 0.05	1.95 ± 0.09*	2.09 ± 0.13*	2.20 ± 0.03*
5	2.10 ± 0.10	2.14 ± 0.05*	2.20 ± 0.15*	2.42 ± 0.01*
6	2.40 ± 0.13	2.55 ± 0.05*	2.82 ± 0.04*	3.21 ± 0.09*

The DCF signal of each dose at each time point was normalized to non-irradiation cells and reported as relative DCF intensity. Each value represents the mean ± S.D. of four independent experiments. Symbols refer significant different from the control group: *, $p < 0.05$ determined by One-way ANOVA.

Table 24 ROS intensity of HaCaT cells after pretreatment with 0.5 mM of silymarin prior to exposed with several doses of UVB and determined by using $DCFH_2$-DA probe.

Time (hour)	Relative DCF intensity			
	0.5 mM SM + 0 J/m^2 (control)	0.5 mM SM + 40 J/m^2	0.5 mM SM + 60 J/m^2	0.5 mM SM + 90 J/m^2
0	1.00 ± 0.01	1.02 ± 0.05	1.06 ± 0.02*	1.18 ± 0.04*
1	1.05 ± 0.02	1.05 ± 0.05	1.28 ± 0.05*	1.30 ± 0.05*
2	1.08 ± 0.02	1.09 ± 0.01	1.34 ± 0.05*	1.48 ± 0.06*
3	1.23 ± 0.01	1.34 ± 0.01*	1.50 ± 0.11*	1.58 ± 0.07*
4	1.38 ± 0.01	1.62 ± 0.07*	1.75 ± 0.28*	1.88 ± 0.07*
5	1.65 ± 0.06	1.80 ± 0.04*	1.90 ± 0.10*	2.02 ± 0.09*
6	2.10 ± 0.05	2.18 ± 0.02*	2.22 ± 0.06*	2.57 ± 0.15*

The DCF signal of each dose at each time point was normalized to non-irradiation cells and reported as relative DCF intensity. Each value represents the mean ± S.D. of four independent experiments. Symbols refer significant different from the control group: *, $p < 0.05$ determined by One-way ANOVA.

Table 25 ROS intensity of HaCaT cells after pretreatment with various concentrations of silymarin prior to exposed 90 J/m^2 UVB and determined by using $DCFH_2$-DA probe.

Time (hour)	Relative DCF intensity			
	control (90J/m^2)	0.01 mM SM + 90J/m^2	0.1 mM SM + 90J/m^2	0.5 mM SM + 90J/m^2
0	1.25 ± 0.01	1.23 ± 0.11	1.19 ± 0.09*	1.18 ± 0.04*
1	1.45 ± 0.01	1.43 ± 0.12	1.35 ± 0.19*	1.30 ± 0.05*
2	1.51 ± 0.01	1.51 ± 0.04	1.48 ± 0.10*	1.48 ± 0.06*
3	1.78 ± 0.01	1.76 ± 0.01	1.73 ± 0.03*	1.58 ± 0.07*
4	2.23 ± 0.01	2.21 ± 0.02	2.20 ± 0.03*	1.88 ± 0.07*
5	2.47 ± 0.03	2.45 ± 0.18	2.42 ± 0.01*	2.02 ± 0.09*
6	3.37 ± 0.01	3.27 ± 0.08*	3.21 ± 0.09*	2.57 ± 0.15*

The DCF signal of each dose at each time point was normalized to non-treated cells and reported as relative DCF intensity. Each value represents the mean ± S.D. of four independent experiments. Symbols refer significant different from the control group: *, $p < 0.05$ determined by One-way ANOVA.

Table 26 ROS intensity of HaCaT cells after pretreatment with various types of antioxidant at concentration of 0.5 mM prior to exposed with 90J/m^2 UVB. The results were determined by $DCFH_2$-DA probe.

Time (hour)	Relative DCF intensity				
	UVB (90J/m^2)	0.5 mM Vit E + 90 J/m^2	0.5 mM Vit C + 90 J/m^2	0.5 mM SM + 90 J/m^2	UVB (0 J/m^2)
0	1.25 ± 0.01	1.12 ± 0.01*	1.13 ± 0.11*	1.18 ± 0.04*	1.18 ± 0.13
1	1.45 ± 0.01	1.20 ± 0.05*	1.31 ± 0.05*	1.30 ± 0.05*	1.27 ± 0.20
2	1.51 ± 0.01	1.39 ± 0.05*	1.47 ± 0.05*	1.48 ± 0.06*	1.35 ± 0.09
3	1.78 ± 0.01	1.47 ± 0.08*	1.52 ± 0.15*	1.58 ± 0.07*	1.43 ± 0.15
4	2.23 ± 0.01	1.74 ± 0.01*	1.82 ± 0.13*	1.88 ± 0.07*	1.70 ± 0.13
5	2.47 ± 0.03	1.91 ± 0.01*	1.93 ± 0.08*	2.02 ± 0.09*	1.80 ± 0.11
6	3.37 ± 0.01	2.19 ± 0.04*	2.21 ± 0.13*	2.57 ± 0.15*	2.09 ± 0.09

The DCF signal of each dose at each time point was normalized to non-treated cells and reported as relative DCF intensity. Each value represents the mean ± S.D. of four independent experiments. Symbols refer significant different from the control group (UVB 90 J/m^2): *, $p < 0.05$ determined by One-way ANOVA.

Table 27 ROS intensity of HaCaT cells after pretreatment with various types of antioxidant at concentration of 0.1 mM prior to exposed with 90J/m^2 UVB. The results were determined by $DCFH_2$-DA probe.

Time (hour)	Relative DCF intensity				
	UVB (90J/m^2)	0.1 mM Vit E + 90 J/m^2	0.1 mM Vit C + 90 J/m^2	0.1 mM SM + 90 J/m^2	UVB (0 J/m^2)
0	1.25 ± 0.01	1.22 ± 0.01	1.24 ± 0.08	1.19 ± 0.09*	1.18 ± 0.13
1	1.45 ± 0.01	1.42 ± 0.05	1.46 ± 0.02	1.35 ± 0.19*	1.27 ± 0.20
2	1.51 ± 0.01	1.48 ± 0.01*	1.51 ± 0.09	1.48 ± 0.10*	1.35 ± 0.09
3	1.78 ± 0.01	1.71 ± 0.02*	1.72 ± 0.13*	1.73 ± 0.03*	1.43 ± 0.15
4	2.23 ± 0.01	2.12 ± 0.06*	2.18 ± 0.17*	2.20 ± 0.03*	1.70 ± 0.13
5	2.47 ± 0.03	2.36 ± 0.05*	2.38 ± 0.06*	2.42 ± 0.01*	1.80 ± 0.11
6	3.37 ± 0.01	3.10 ± 0.01*	3.11 ± 0.15*	3.21 ± 0.09*	2.09 ± 0.09

The DCF signal of each dose at each time point was normalized to non-treated cells and reported as relative DCF intensity. Each value represents the mean ± S.D. of four independent experiments. Symbols refer significant different from the control group (UVB 90 J/m^2): *, $p < 0.05$ determined by One-way ANOVA.

Table 28 ROS intensity of HaCaT cells after pretreatment with several types of antioxidant at concentration of 0.5 mM prior to exposed with 90 J/m^2 of UVB. The results were determined using $DCFH_2$-DA probe. This result was used for finding kinetics of antioxidant. Each value represents the mean ± S.D. of four independent experiments.

Time (hour)	Relative DCF intensity				
	UVB (90J/m^2)	0.5 mM Vit E + 90 J/m^2	0.5 mM Vit C + 90 J/m^2	0.5 mM SM + 90 J/m^2	UVB (0 J/m^2)
0	1.20 ± 0.01	1.17 ± 0.10	1.18 ± 0.02	1.19 ± 0.01	1.16 ± 0.07
0.5	1.29 ± 0.02	1.21 ± 0.12	1.25 ± 0.02	1.27 ± 0.01	1.19 ± 0.05
1	1.36 ± 0.08	1.25 ± 0.03	1.30 ± 0.02	1.33 ± 0.01	1.23 ± 0.09
1.5	1.43 ± 0.08	1.29 ± 0.08	1.37 ± 0.03	1.41 ± 0.04	1.27 ± 0.01
2	1.50 ± 0.09	1.35 ± 0.09	1.43 ± 0.03	1.48 ± 0.02	1.30 ± 0.03
3	1.79 ± 0.04	1.49 ± 0.03	1.59 ± 0.05	1.63 ± 0.04	1.48 ± 0.01
4	2.24 ± 0.03	1.75 ± 0.04	1.83 ± 0.05	1.89 ± 0.05	1.75 ± 0.04
5	2.65 ± 0.10	1.97 ± 0.04	2.03 ± 0.01	2.19 ± 0.02	2.10 ± 0.04
6	3.39 ± 0.12	2.29 ± 0.02	2.39 ± 0.09	2.60 ± 0.03	2.35 ± 0.05

Table 29 The kinetic constant of ROS production and the percentage of cell viability.

At 24 hours	K of ROS	Cell viability (%)
Control (0 J/m^2)	0.2695	100
40 J/m^2	0.5054	77.89
60 J/m^2	0.5484	58.72
90 J/m^2	0.6376	51.89

These results were used for correlation between kinetic constant of ROS and cell viability. Each value represents the mean ± S.D. of four independent experiments.

Table 30 The kinetic constant of ROS production and the percentage of apoptosis.

At 24 hours	K of ROS	Apoptosis (%)
Control (0 J/m^2)	0.2695	0
40 J/m^2	0.5054	45.58
60 J/m^2	0.5484	56.01
90 J/m^2	0.6376	78.43

These results were used for correlation between kinetic constant of ROS and apoptosis. Each value represents the mean ± S.D. of four independent experiments.

VITA

Miss Apiriya Dhumrongvaraporn was born on June 16, 1988 in Bangkok. She received her B.Sc. in Applied Chemistry from the Faculty of Science, Chulalongkorn University in 2010.